Tissue Antigens ISSN 0001-2815

Identification of HLA-A*3101-restricted cytotoxic T-lymphocyte response to human immunodeficiency virus type 1 (HIV-1) in patients with chronic HIV-1 infection

M. A. Borghan[1], S. Oka[2] & M. Takiguchi[1]

1 Division of Viral Immunology, Center for AIDS Research, Kumamoto University, Kumamoto, Japan
2 AIDS Clinical Center, International Medical Center of Japan, Tokyo, Japan

Key words
CTL; epitope; HIV-1; HLA-A*3101; peptide

Correspondence
Masafumi Takiguchi
Division of Viral Immunology
Center for AIDS Research
Kumamoto University
2-2-1 Honjo
Kumamoto 860-0811
Japan
e-mail: masafumi@kaiju.medic.kumamoto-u.ac.jp

Received 25 May 2005; revised 21 July 2005; accepted 3 August 2005

doi: 10.1111/j.1399-0039.2005.00489.x

Abstract

Virus-specific cytotoxic T-lymphocyte (CTL) responses are critical in the control of human immunodeficiency virus type 1 (HIV-1) infections. As several HIV-1 CTL epitopes restricted to many HLA types are already known, we aimed at identifying the CTL epitopes restricted by HLA-A*3101 in an effort to expand the epitope repertoire available for the development of potential T cell-mediated therapeutic measures and protective vaccines. Scanning of HIV-1 clade B SF2 strain proteins for the presence of peptides containing HLA-A*3101-binding motifs revealed 88 nine- to 11-mer peptides that had been synthesized and assayed for binding to HLA-A*3101 molecules. Peptides with medium to high HLA-binding affinity were tested for their ability to stimulate a CTL response in the peripheral blood mononuclear cells (PBMCs) from selected HIV-1-infected patients. Two of these binding peptides, Env769–779 (RLRDLLLIAAR) and Nef192–200 (KLAFHHMAR), induced peptide-specific CTLs in PBMCs from at least two of five HIV-1-seropositive individuals. CTL clones specific for the two peptides killed HLA-A*3101-expressing target cells infected with HIV-1 recombinant vaccinia virus, indicating that these peptides were naturally processed HLA-A*3101-restricted CTL epitopes. Identification of T-cell epitopes on HIV-1 proteins will increase our understanding of the role of $CD8^+$ T cells in HIV-1 infections and assist in the design of new protective strategies.

Introduction

Human immunodeficiency virus type 1 (HIV-1)-specific cytotoxic T lymphocytes (CTLs) are considered to play a central role in the immune response against HIV-1 (1–3). High levels of HIV-1-specific CTLs are detectable in subjects with asymptomatic chronic infection (4–8), but their level generally declines with disease progression (9). Furthermore, *in vitro* studies have demonstrated potent inhibition of viral replication by HIV-1-specific CTL, mediated by both lytic and non-lytic mechanisms (10); and *in vivo*, there is strong evidence that AIDS viruses evolve to escape CTL recognition by undergoing epitope-specific mutations (11–14). The critical role of virus-specific CTL responses for the control of viraemia has been directly demonstrated by $CD8^+$ T-cell depletion studies in simian immunodeficiency virus infection in macaques, which show that $CD8^+$ T cells effectively suppress viral replication (15, 16). Recent data derived from HIV-1-infected individuals who were treated during an acute HIV-1 infection showed enhancement of both CTL and T-helper cell responses against HIV-1 associated with subsequent viral control following supervised treatment interruptions (17). These data suggest that the induction of HIV-1-specific CTL responses *in vivo* may help prevent infection of normal individuals or attenuate HIV-1 disease in infected individuals.

The precise characterization of epitope-specific CTL responses is important for assessing HIV pathogenesis and vaccine candidates. However, viral escape from CTL recognition may limit the durability of the potential

protection afforded by such vaccines (18, 19). Moreover, association of escape mutations with particular host HLA class I alleles (20) may further confine the use of universal vaccines and support the development of population-based vaccines. To achieve this goal, we need to identify and characterize CTL epitopes restricted to particular HLA class I alleles in a given area.

HLA-A31 is one of the common alleles in Asia (21). Of the 12 reported HLA-A31 subtypes (A*3101–A*3112) (IMGT/HLA database: http://www.ebi.ac.uk/imgt/hla) (22), HLA-A*3101 is the most common (21). Therefore, the identification of HLA-A*3101-restricted HIV-1 epitopes is important in studies of immunopathogenesis and for vaccine development in Asia. We previously showed reverse immunogenetics to be a useful method to identify HIV-1-specific CTL epitopes presented by HLA-A*2402, HLA-A*2601, HLA-A*3303 and HLA-B*5101 (23–26). In this study, potential epitopes were identified by scanning HIV-1 proteins for peptides containing the HLA-A*3101 motif. Peptide-specific $CD8^+$ T cells were measured by counting interferon-γ (IFN-γ)-producing $CD8^+$ T cells after stimulating peripheral blood mononuclear lymphocytes (PBMCs) from HIV-1-infected HLA-A*3101$^+$ individual with HLA-A*3101-binding HIV-1 peptides. $CD8^+$ T-cell epitopes were finally identified by testing whether peptide-specific $CD8^+$ T-cell clones could kill target C1R-A*3101 cells infected with HIV-1 recombinant (r-HIV-1) vaccinia virus.

Materials and methods

Patients

Blood samples were collected with informed consent from five HLA-A*3101$^+$ individuals with HIV-1 infection (KI-033, KI-039, KI-126, KI-147 and KI-178).

Cells

RMA-S cells expressing HLA-A*3101 (RMA-S-A*3101) were previously generated (22). C1R cells expressing HLA-A*3101 (C1R-A*3101) were generated by transfecting C1R cells, which express HLA-Cw4 and HLA-B*3503, with the HLA-A*3101 gene. C1R-A*3101 and RMA-S-A*3101 cells were maintained in RPMI-1640 medium containing 10% foetal calf serum (FCS) and 0.15 mg/ml of hygromycin B. C1R and RMA-S cells were cultured in RPMI-1640 medium supplemented with 10% FCS.

Synthetic peptides

Sequences derived from proteins of HIV-1 SF2 strain were screened for HLA-A*3101-binding motifs. Peptides were prepared by an automated multiple peptide synthesizer and examined by high-performance liquid chromatography and mass spectrometry (HiPep Laboratories, Kyoto, Japan). Peptides with more than 90% purity were used in this study (Table 1).

HLA stabilization assay

Binding of HIV-1-derived peptides to HLA-A*3101 was examined by the HLA stabilization assay as previously described (22). Briefly, RMA-S-A*3101 cells were cultured for 16 h at 26°C and then pulsed with peptides (10^{-3}–10^{-7} M) for 1 h at 26°C. After further incubation for 3 h at 37°C, the peptide-pulsed cells were stained with anti-HLA class I α3 domain-specific monoclonal antibody TP25.99 (a generous gift from Dr S. Ferrone, Roswell Park Cancer Institute Buffallow, NY) followed by fluorescein isothiocyanate-conjugated IgG fraction of sheep anti-mouse immunoglobulin (Silenius Laboratories, Hawthorn, Victoria, Australia). The mean fluorescence intensity (MFI) was measured by flow cytometry (FACS Calibur; BD Biosciences, San Jose, CA). The MFI of RMA-S-A*3101 cells was obtained by subtracting the MFI value of RMA-S-A*3101 cells incubated for 3 h at 37°C from that of control cells cultured at 26°C. HLA-A*3101-binding peptides were defined as those that at a concentration of 10^{-3} M caused >25% increase in MFI compared with control RMA-S-A*3101 cells cultured at 26°C. The peptide concentration that yielded the half-maximal MFI level (BL_{50} value) was calculated. Binding peptides were classified into three categories according to their BL_{50}: high binding ($BL_{50} < 10^{-5}$ M), medium binding (BL_{50} 10^{-5}–10^{-4} M) and low binding ($BL_{50} \geq 10^{-4}$ M) (Table 1).

Detection of peptide-specific interferon-γ-producing $CD8^+$ T cells in PBMCs from HIV-1-infected HLA-A*3101$^+$ individuals

PBMCs (5×10^5) from HIV-1-seropositive or HIV-1-seronegative individuals expressing HLA-A*3101 were stimulated with HLA-A*3101-binding peptides. After 10–14 days of culture, IFN-γ production activity was determined by flow cytometry. Briefly, bulk cultures were stimulated by C1R-A*3101 cells pulsed with the corresponding peptide cocktail or individual peptide (1 μM) for 2 h at 37°C (Table 2). Brefeldin A (10 μg/ml) was then added, and the culture was continued for an additional 4 h. The cells were then collected and stained with anti-CD8 monoclonal antibody (Dako Corporation, Glostrup, Denmark). After having been treated with 4% paraformaldehyde solution, the cells were permeabilized in permeabilization buffer [0.1% saponin and 20% newborn calf serum (NCS) in phosphate-buffered saline] at 4°C for 10 min and stained with anti-IFN-γ monoclonal antibody (PharMingen, San Diego, CA). After thorough washing with the permeabilization buffer, the cells were analysed by flow cytometry (FACS Calibur; BD Biosciences).

Table 1 HLA-A *3101-binding HIV-1 SF2-derived peptides

Peptide	Protein	Sequence	BL_{50}
SF2-Env373–381	Env	IVMHSFNCR	8.1×10^{-6}
SF2-Env769–779	Env	RLRDLLLIAAR	1.2×10^{-5}
SF2-Env835–845	Env	AYRAILHIHRR	1.3×10^{-5}
SF2-Env835–844	Env	AYRAILHIHR	1.4×10^{-5}
SF2-Env827–837	Env	RVIEVAQRAYR	1.8×10^{-5}
SF2-Env193–201	Env	NYRLIHCNR	1.9×10^{-5}
SF2-Env568–578	Env	TVWGIKQLQAR	2.5×10^{-5}
SF2-Env761–769	Env	SLCLFSYRR	2.6×10^{-5}
SF2-Env578–587	Env	RVLAVERYLR	2.7×10^{-5}
SF2-Env696–706	Env	IVFAVLSIVNR	3.5×10^{-5}
SF2-Env574–584	Env	QLQARVLAVER	3.6×10^{-5}
SF2-Env579–587	Env	VLAVERYLR	3.7×10^{-5}
SF2-Env763–771	Env	CLFSYRRLR	4.1×10^{-5}
SF2-Env761–771	Env	SLCLFSYRRLR	4.2×10^{-5}
SF2-Env699–708	Env	AVLSIVNRVR	4.2×10^{-5}
SF2-Env839–847	Env	ILHIHRRIR	1.0×10^{-4}
SF2-Env464–474	Env	EVFRPGGGDMR	$>10^{-3}$
SF2-Env247–255	Env	TVQCTHGIR	$>10^{-3}$
SF2-Env758–768	Env	DLRSLCLFSYR	$>10^{-3}$
SF2-Env710–719	Env	GYSPLSFQTR	$>10^{-3}$
SF2-Env531–541	Env	AVSLTLTVQAR	$>10^{-3}$
SF2-Env700–708	Env	VLSIVNRVR	$>10^{-3}$
SF2-Env547–556	Env	IVQQQNNLLR	$>10^{-3}$
SF2-Env719–728	Env	RLPVPRGPDR	$>10^{-3}$
SF2-Pol60–70	Pol	TLWQRPLVTIR	1.6×10^{-5}
SF2-Pol430–439	Pol	KVKQLCKLLR	1.7×10^{-5}
SF2-Pol228–238	Pol	KLVDFRELNKR	3.0×10^{-5}
SF2-Pol813–822	Pol	AYFLLKLAGR	4.3×10^{-5}
SF2-Pol894–902	Pol	AVFIHNFKR	8.4×10^{-5}
SF2-Pol974–984	Pol	VVPRRKAKIIR	$>10^{-3}$
SF2-Gag30–39	Gag	KLKHIVWASR	6.4×10^{-6}
SF2-Gag34–43	Gag	IVWASRELER	9.2×10^{-6}
SF2-Gag144–152	Gag	MVHQAISPR	7.8×10^{-5}
SF2-Gag81–91	Gag	TVATLYCVHQR	$>10^{-3}$
SF2-Gag298–307	Gag	YVDRFYKTLR	$>10^{-3}$
SF2-Gag278–288	Gag	MYSPTSILDIR	$>10^{-3}$
SF2-Gag484–492	Gag	ELYPLTSLR	$>10^{-3}$
SF2-Gag297–307	Gag	DYVDRFYKTLR	$>10^{-3}$
SF2-Gag354–363	Gag	GVGGPGHKAR	$>10^{-3}$
SF2-Nef192–200	Nef	KLAFHHMAR	8.9×10^{-5}
SF2-Nef73–81	Nef	PVRPQVPLR	1.6×10^{-4}
SF2-Nef100–110	Nef	GLEGLIWSQRR	$>10^{-3}$
SF2-Vif9–19	Vif	IVWQVDRMRIR	5.3×10^{-6}
SF2-Vif165–173	Vif	SVKKLTEDR	8.9×10^{-6}
SF2-Vif6–15	Vif	QVMIVWQVDR	3.5×10^{-5}
SF2-Vif1–9	Vif	IVWQVDRMR	8.8×10^{-5}
SF2-Vif124–132	Vif	ILGYRVSPR	2.1×10^{-4}
SF2-Vif80–90	Vif	HLGQGVAIEWR	$>10^{-3}$
SF2-Vif68–77	Vif	TYWGLHTGER	$>10^{-3}$
SF2-Tat42–52	Tat	GLGISYGRKKR	$>10^{-3}$
SF2-Tat46–55	Tat	SYGRKKRRQR	$>10^{-3}$
SF2-Tat46–56	Tat	SYGRKKRRQRR	$>10^{-3}$
SF2-Tat68–78	Tat	SLSKQPASQSR	$>10^{-3}$
SF2-Vpu26–35	Vpu	VLIEYRKILR	3.5×10^{-5}
SF2-Vpu25–35	Vpu	IVLIEYRKILR	$>10^{-3}$
SF2-Vpr63–73	Vpr	ILQQLLFIHFR	5.2×10^{-5}

HIV-1, human immunodeficiency virus type 1.

Table 2 Induction of peptide cocktail-specific $CD8^+$ T cells in bulk cultures

Peptide cocktail	Percentage of $CD8^+$ IFN-γ^+ cells	
	KI-033	KI-126
Cocktail 1 (Env373–381, Gag30–39, Gag34–43)	0	0
Cocktail 2 (Gag144–152, Pol894–902, Nef192–200)	2.8	13.2
Cocktail 3 (Env699–708, Env761–771, Env763–771, Pol813–822)	0	0
Cocktail 4 (Env696–706, Env574–584, Env579–587)	0	0
Cocktail 5 (Env568–578, Env578–587, Env761–769, Pol228–238)	0	0
Cocktail 6 (Env193–201, Env827–837, Env835–844, Pol430–439)	0	0
Cocktail 7 (Env835–845, Env839–847, Env769–779, Nef73–81)	8.7	68.5

IFN-γ, interferon-γ.

Generation of CTL clones

Nef192–200-specific and Env769–779-specific CTL clones were generated from an established peptide-specific bulk CTL culture by limiting dilution in 96-well U-bottomed microtiter plates (Nunc, Roskilde, Denmark) by using the following cloning mixture: RPMI-1640 medium supplemented with 10% FCS and recombinant human interleukin-2 (200 U/ml; Ajinomoto, Tokyo, Japan), 1×10^6 irradiated allogeneic PBMCs from a healthy donor and 1×10^5 irradiated C1R-A*3101 cells pulsed with the corresponding peptide (1 μM). Wells positive for growth after about 14 days were tested for cytolytic activity by the ^{51}Cr-release assay described below.

CTL assay

The cytotoxic activity of CTL clone was determined by using a standard ^{51}Cr-release assay. C1R-A*3101 cells (2×10^5) were first incubated with 100 μCi $Na_2{}^{51}CrO_4$ (PerkinElmer, Boston, MA) in saline for 1 h at 37°C and then washed three times with RPMI-1640 medium containing 10% NCS. The ^{51}Cr-labelled cells (2×10^3) were pulsed with the corresponding peptide (1 μM) for 1 h at 37°C, after which a CTL clone (4×10^3) was added and incubation was continued further for 4 h at 37°C. A portion of the culture supernatant (100 μl) was then removed and analysed by a γ counter (Perkin Elmer, CT). The percentage of specific lysis was calculated as described previously (25). In another experiment, labelled C1R-A*3101 cells were pulsed with various concentrations (10^3–0.1 nM) of the corresponding peptide.

Confirmation of epitope authenticity by cytotoxic assay

C1R-A*3101 cells were infected for 12–18 h with 10 plaque-forming units of either recombinant vaccinia virus expressing a given protein (Env or Nef) or wild-type Vaccinia. The infected cells (2×10^5) were then labelled with 100 μCi $Na_2{}^{51}CrO_4$ in saline, washed three times and used as target cells in the cytotoxic assay described above. The activities of CTL clones against recombinant vaccinia virus-infected target cells were tested at an effector : target ratio of 4:1.

Results

Identification of HLA-A*3101-binding peptides derived from HIV-1 SF2 proteins

Nine- to 11-mer peptide sequences with two anchor residues of HLA-A*3101 peptides (Leu, Phe, Tyr or Val at position 2 and Arg at the C terminus) (27) were selected from the amino acid sequence of different HIV-1 SF2 strains, and then 88 peptides matched to these sequences were synthesized. The binding affinity of the synthesized peptides for HLA-A*3101 molecule was tested by conducting a stabilization assay using RMA-S-A*3101 cells (22). Fifty-six of the 88 peptides bound to HLA-A*3101 (Table 1). Among these binding peptides, five peptides were high binders ($BL_{50} < 10^{-5}$ M), 25 peptides were medium binders (BL_{50} 10^{-5} to $<10^{-4}$ M) and 26 peptides were low binders ($BL_{50} \geq 10^{-4}$ M). Peptides with high or medium binding affinity to HLA-A*3101 were then grouped into cocktails and used to induce CTLs in PBMCs from HIV-1-infected individuals expressing HLA-A*3101.

Induction of HIV-1 peptide-specific $CD8^+$ T cells from PBMCs of HLA-A*3101$^+$ HIV-1-infected individuals

PBMCs from two HLA-A*3101$^+$ HIV-1-seropositive individuals (KI-033 and KI-126) were stimulated *in vitro* with HLA-A*3101-binding peptide cocktails for 10–14 days. IFN-γ production by each bulk culture in response to C1R-A*3101 prepulsed with the corresponding peptide cocktail was assessed by intracellular staining. Bulk cultures from both KI-033 and KI-126 responded specifically to cocktails 2 and 7, as summarized in Table 2. Cocktail 2 induced a relatively low number of IFN-γ-producing $CD8^+$ T cells in bulk cultures from both patients KI-033 and KI-126 (2.8 and 13.2%, respectively). By contrast, cocktail 7 markedly induced a high number of IFN-γ-producing $CD8^+$ T cells, particularly in the bulk culture

from KI-126 (68.5%). To determine the peptide(s) responsible for the specific response to each cocktail, we stimulated the bulk cultures with C1R-A*3101 prepulsed with single peptides. Two peptides, Nef192–200 and Env769–779, induced $CD8^+$ T cells to produce IFN-γ in both patients KI-033 and KI-126 (Figure 1).

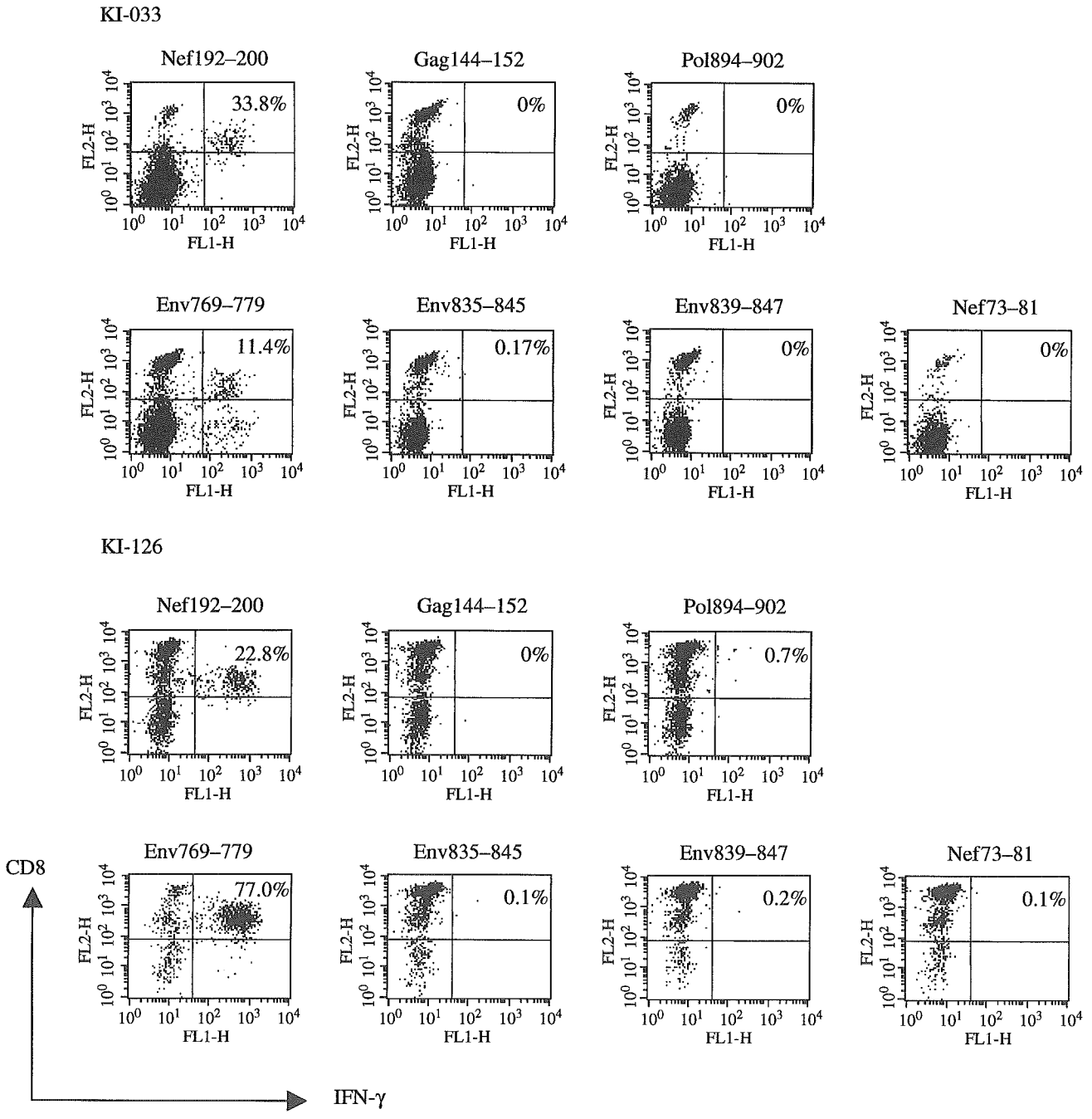

Figure 1 Induction of HIV-1-specific $CD8^+$ T cells from PBMCs of HIV-1-infected individuals bearing HLA-A*3101. PBMCs from patients KI-033 and KI-126 were stimulated *in vitro* with HLA-A*3101-binding peptide cocktails (Table 2) and were then cultured for 10–14 days. After the cultured PBMCs had been stimulated with the peptide cocktail-prepulsed C1R-A*3101 cells for 6 h, the number of IFN-γ-producing $CD8^+$ T cells was measured by flow cytometry. Cultured cells containing IFN-γ-producing $CD8^+$ T cells were again stimulated with C1R-A*3101 cells prepulsed with the individual peptides comprising cocktails 2 and 7, followed by intracellular IFN-γ staining. Percentages in upper right quadrants indicate IFN-γ-producing $CD8^+$ T cells. HIV-1, human immunodeficiency virus type 1; IFN, interferon; PBMCs, peripheral blood mononuclear cells.

Identification of HIV-1-specific CD8$^+$ T-cell epitopes endogenously processed and presented by HLA-A*3101

In order to further analyse these two peptides, we generated CTL clones specific for Nef192–200 and Env769–779 from patients KI-033 and KI-126, respectively. These CTL clones were capable of killing C1R-A*3101 cells pulsed with the corresponding peptide in a concentration-dependent manner (Figure 2).

To clarify whether these two peptides were endogenously processed and presented by HLA-A*3101, we investigated the ability of these CTL clones to kill C1R-A*3101 cells infected with recombinant vaccinia virus expressing the HIV-1 Nef or Env protein. The CTL clones effectively killed C1R-A*3101 cells infected with the recombinant vaccinia virus, but not those cells infected with wild-type vaccinia virus or uninfected cells (Figure 3). These results indicate that Nef192–200 and Env769–779 are naturally processed HLA-A*3101-restricted CTL epitopes.

Detection of Env769–779-specific and Nef192–200-specific CD8$^+$ T cells in chronically HIV-1-infected individuals

To investigate whether CD8$^+$ T cells specific for Nef192–200 and Env769–779 epitopes could be frequently found in HLA-A*3101$^+$ HIV-1-infected individuals, we expanded our investigation to include three more patients (KI-039, KI-147 and KI-178) by stimulating their PBMCs with epitope peptides. Env769–779-specific CD8$^+$ T cells were observed in the bulk culture from only one (KI-039) of these three patients (Table 3). No Nef192–200-specific CD8$^+$ T cells were induced in any of these individuals. Taken together, our data indicate that Env769–779-specific and Nef192–200-specific CD8$^+$ T cells were detected in the cultures from three and two of HLA-A*3101$^+$ HIV-1-infected individuals, respectively.

Discussion

This study focused on the identification and characterization of HIV-1-derived CTL epitopes restricted by the HLA-A*3101 allele. Fifty-six HLA-A*3101-binding peptides were identified based on their strong binding to HLA-A*3101 molecules. These peptides were tested for specific recognition by CTLs in five HIV-1-infected individuals and four HIV-1-seronegative controls expressing the HLA-A*3101 allele. Two of the 56 HLA-A*3101 binders induced peptide-specific T-cell responses in at least two HIV-1-infected subjects. Our results include the first description of HLA-A*3101-restricted CTL epitope Nef192–200. The other epitope, Env769–779, was a variant version of the previously described HLA-A3.1- and HLA-A31-restricted CTL epitope (28, 29).

While the association between the peptide-binding motif and the amino acid sequence of the actual CTL epitopes is not always absolute (30–32), the identification of two HLA-A*3101-restricted HIV-1 CTL epitopes in this study provides further evidence that the prediction of CTL epitopes from the binding motif of the corresponding HLA class I molecule is an efficient approach for epitope identification. Previous pool sequencing analysis showed that peptide binding to HLA-A*3101 molecule requires Arg as the C-terminal anchor and four possible hydrophobic residues, Leu, Phe, Tyr or Val, as the P2 anchor (33). Using the HLA stabilization assay, we further demonstrated that positively charged P1 residues have a positive effect on the binding of epitope peptides to HLA-A*3101 molecules (33). When the sequence of the Env769–779 epitope (RLRDLLLIAAR) is compared to that of the

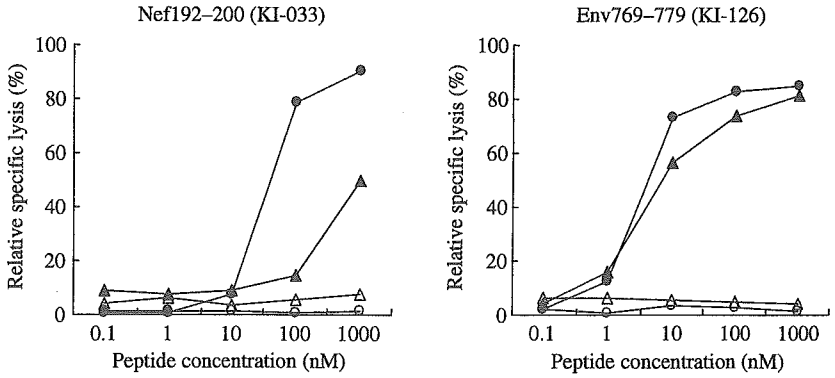

Figure 2 Recognition of HIV-1 Nef and Env peptides by established CTL clones. The CTL activity of Nef192–200-specific and Env769–779-specific clones against target cells pulsed with 10-fold serial dilution of the corresponding peptide was tested at an effector : target (E : T) ratio of 4:1. C1R-A*3101 cells (closed symbols) and C1R cells (open symbols) were used as target cells. Two CTL clones (circle and triangle) were tested for each epitope. Nef192–200-specific and Env769–779-specific CTL clones were established from KI-033 and KI-126, respectively. HIV-1, human immunodeficiency virus type 1; CTL, cytotoxic T lymphocyte.

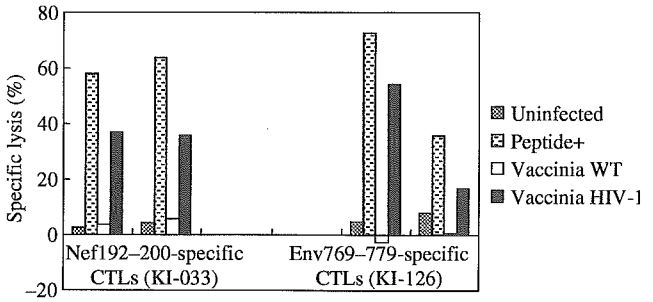

Figure 3 Recognition of HIV-1 epitopes presented on C1R-A*3101 cells infected with HIV-1 recombinant vaccinia virus. The CTL activity of Nef192–200-specific and Env769–779-specific clones against C1R-A*3101 cells prepulsed with 1 μM of epitope peptide (peptide$^+$) or infected with recombinant vaccinia virus (vaccinia HIV-1) expressing the corresponding HIV-1 protein, Nef or Env, or wild-type vaccinia virus (vaccinia WT) was tested at an effector : target (E : T) ratio of 4:1. HIV-1, human immunodeficiency virus type 1; CTL, cytotoxic T lymphocyte.

Nef192–200 epitope (KLAFHHMAR), both epitopes have a positively charged residue, Arg and Lys, respectively, at P1. These epitope peptides also bound to HLA-A*3101 molecules with high and medium affinity, respectively (Table 1). These results further support the importance of positively charged P1 residues in HLA-A*3101-binding peptides.

An increasing body of data demonstrates that virus-specific CTL responses play a crucial role in the immune response against HIV-1 (1, 3). Vaccines inducing strong CTL responses against HIV-1 may therefore represent a possible avenue to prevent infection or attenuate HIV-1 disease. However, the large degree of HLA polymorphism represents a significant challenge for this approach, if specific epitopes for a large number of different HLA class I specificities have to be defined. The identification of peptides capable of binding to common HLA class I molecules in a nonethically biased population may simplify the epitope selection with potential practical implications for development of epitope-based vaccines and immunotherapy. This study therefore focused on the identification of CTL epitopes that have high binding affinities for the HLA-A*3101 molecule, which is a common allele in Asia (9.3% in the Japanese population) (33, 34). CTL responses against the identified HLA-A*3101 binders were analysed in Japanese individuals expressing predominately HLA-A*3101. Our data obtained from individuals who were treated shortly after an acute HIV-1 infection demonstrate that both epitopes were recognized during the initial CTL response and suggest that they might subsequently participate in the early control of viraemia. However, it is important to assess whether these CTL clones are able to recognize the autologous virus.

As Nef is an early regulatory protein which is not expressed in infectious particles, the Nef-specific CTL response could play a critical role in host cytotoxic defences against infected cells at an early step of the HIV-1 replication. We report here a new HLA-A*3101-restricted Nef epitope (aa 192–200) located at the carboxyl-terminal region of the Nef protein, which is recognized by CTL in the context of many HLA molecules such as A1 and B35 (35). This region appears to be particularly interesting with respect to vaccine development, because it has been previously reported to be an immunodominant region for T helper cell and antibody responses (36).

The induction of the two types of epitope-specific CD8$^+$ T cells varied among five HIV-1-infected individuals expressing HLA-A*3101 (Table 3). Env769–779-specific and Nef192–200-specific CD8$^+$ T cells were found in three and two of them, respectively. These results indicate that CD8$^+$ T cells specific for these epitopes, particularly Env769–779, were frequently induced in HLA-A*3101$^+$ HIV-1-infected individuals. However, the induction of these HIV-1-specific CD8$^+$ T cells was correlated neither with viral load nor with CD4$^+$ or CD8$^+$ T cell number. For those subjects in whom these CTL responses were not

Table 3 Induction of epitope-specific CD8$^+$ T cells among PBMCs from HLA-A*3101$^+$ HIV-1-infected individuals

				Percentage of IFN-γ-producing cells in CD8$^+$ T cells	
Patients	Viral load[a]	CD4[b]	CD8[b]	Nef192–200	Env769–779
KI-033	4.3×10^5	225	578	33.8	11.4
KI-039	2.4×10^4	646	850	0	4.2
KI-126	2.1×10^4	524	883	22.8	77.0
KI-147	7.2×10^3	169	434	0	0
KI-178	9.9×10^4	407	1544	0	0
HIV-1-seronegative individuals ($n = 4$)				0.4 ± 0.3	0.5 ± 0.4

HIV-1, human immunodeficiency virus type 1; IFN-γ interferon-γ PBMCs, peripheral blood mononuclear cells.
[a]Copies/ml.
[b]Cells/l.

Table 4 Variation in HLA-A*3101-restricted epitopes in clades A–E

Epitope	Sequence											Clade A	Clade B	Clade C	Clade D	Clade E
Nef192–200	K	L	A	F	H	H	M	A	R			0/10	2/40	0/19	0/21	0/16
	R	–	–	–	–	–	–	–	–			0/10	26/40	0/19	0/21	0/16
	R	–	–	–	–	–	V	–	–			0/10	12/40	0/19	0/21	0/16
	R	–	–	–	E	–	K	–	–			0/10	0/40	0/19	21/21	0/16
	S	–	–	R	R	–	L	–	–			0/10	0/40	19/19	0/21	1/16
	A	–	–	R	K	–	I	–	–			0/10	0/40	0/19	0/21	15/16
Env769–779	R	L	R	D	L	L	L	I	A	A	R	0/29	9/52	3/22	6/26	0/19
	–	–	–	–	F	I	–	–	–	–	–	25/29	0/52	12/22	0/26	19/19
	–	–	–	–	–	–	–	–	V	T	–	0/29	28/52	1/22	1/26	0/19
	–	–	–	–	–	–	–	–	V	–	–	0/29	15/52	0/22	0/26	0/19
	–	–	–	–	–	I	–	–	–	–	–	4/29	0/52	5/22	7/26	0/19
	–	–	–	–	–	I	–	–	–	T	–	0/29	0/52	1/22	12/26	0/19

observed (KI-147 and KI-178), autologous virus sequencing should reveal whether escape mutations can account for the absence of these CTLs.

We searched reported HIV-1 sequences of clades A–E (HIV sequence database, Los Alamos, NM) for major variants of these epitopes. The sequences of Env769–779 (RLRDLLLIAAR) and Nef192–200 (KLAFHHMAR) were found in nine of 52 and two of 40 HIV-1 clade B isolates, respectively. The Env769–779 sequence was also found in clades D and C (Table 4). These sequences were rarely or not found in isolates of clades A, C, D and E. However, epitope variants with one or two amino acid changes were predominantly found among HIV-1 isolates. An Env769–779 mutant carrying Phe and Ile at positions 5 and 6, respectively, was a predominant sequence in clades A and E, whereas one carrying Val and Thr in positions 9 and 10, respectively, was frequently found in clade B. On the other hand, a Nef192–200 mutant carrying Arg at position 1 alone or with Val at position 7 was a common variant in clade B. At least three amino acid changes within this epitope were observed as major variants in clades C, D and E (Table 4). Given that amino acid changes in both epitope variants do not affect the anchor residues, it would be interesting to investigate whether the established CTL clones can recognize those epitope variants. Given that the two anchor residues (P2 and C-terminus) are conserved for these two epitopes among all HIV-1 isolates, it is tempting to assess the effect of predominant amino acid changes in these epitopes on their binding to HLA-A*3101 molecule and CTL recognition.

In conclusion 56 peptides were identified based on their binding to the HLA-A*3101 allele. Two of these peptides, including a variant of the previously described CTL epitope on HIV-1 Env, were recognized by CTL in acutely HIV-1-infected individuals. Further studies are needed to determine at what level the individual epitope-specific CTL response contributes to the entire CTL response in infected individuals so that we can assess whether these epitopes would be useful for the development of prophylactic or therapeutic vaccines.

Acknowledgments

The authors thank Dr S. Ferrone for the gift of monoclonal antibody TP25.99 and Sachiko Sakai for secretarial assistance. This work was supported by a grant-in-aid for scientific research from the Ministry of Health, Labour and Welfare, the Government of Japan; by a grant from the Japan Health Science Foundation; and by a grant from the Organization for Pharmaceutical Safety and Research.

References

1. Altfeld M, Rosenberg ES. The role of CD4(+) T helper cells in the cytotoxic T lymphocyte response to HIV-1. *Curr Opin Immunol* 2000: **12**: 375–80.
2. Brander C, Walker BD. T lymphocyte responses in HIV-1 infection: implications for vaccine development. *Curr Opin Immunol* 1999: **11**: 451–9.
3. Goulder PJ. Anti-HIV cellular immunity: recent advances towards vaccine design. *AIDS* 1999: **13** (Suppl. A): S121–36.
4. Harrer E, Harrer T, Buchbinder S et al. HIV-1-specific cytotoxic T lymphocyte response in healthy, long-term non-progressing seropositive persons. *AIDS Res Hum Retroviruses* 1994: **10**: S77–8.
5. Harrer T, Harrer E, Kalams SA et al. Cytotoxic T lymphocytes in asymptomatic long-term nonprogressing HIV-1 infection. Breadth and specificity of the response and relation to in vivo viral quasispecies in a person with prolonged infection and low viral load. *J Immunol* 1996: **156**: 2616–23.
6. Harrer T, Harrer E, Kalams SA et al. Strong cytotoxic T cell and weak neutralizing antibody responses in a subset of persons with stable nonprogressing HIV type 1 infection. *AIDS Res Hum Retroviruses* 1996: **12**: 585–92.
7. Rinaldo C, Huang XL, Fan ZF et al. High levels of anti-human immunodeficiency virus type 1 (HIV-1) memory cytotoxic T-lymphocyte activity and low viral load are

associated with lack of disease in HIV-1-infected long-term nonprogressors. *J Virol* 1995: **69**: 5838–42.
8. Walker BD, Chakrabarti S, Moss B et al. HIV-specific cytotoxic T lymphocytes in seropositive individuals. *Nature* 1987: **328**: 345–8.
9. Klein MR, Van Baalen CA, Holwerda AM et al. Kinetics of Gag-specific cytotoxic T lymphocyte responses during the clinical course of HIV-1 infection: a longitudinal analysis of rapid progressors and long-term asymptomatics. *J Exp Med* 1995: **181**: 1365–72.
10. Yang OO, Walker BD. $CD8^+$ cells in human immunodeficiency virus type I pathogenesis: cytolytic and noncytolytic inhibition of viral replication. *Adv Immunol* 1997: **66**: 273–311.
11. Allen TM, O'Connor DH, Jing P et al. Tat-specific cytotoxic T lymphocytes select for SIV escape variants during resolution of primary viraemia. *Nature* 2000: **407**: 386–90.
12. Evans DT, O'Connor DH, Jing P et al. Virus-specific cytotoxic T-lymphocyte responses select for amino-acid variation in simian immunodeficiency virus Env and Nef. *Nat Med* 1999: **5**: 1270–6.
13. Koenig SA, Conley J, Brewah YA et al. Transfer of HIV-1-specific cytotoxic T lymphocytes to an AIDS patient leads to selection for mutant HIV variants and subsequent disease progression. *Nat Med* 1995: **1**: 330–6.
14. Price DA, Goulder PJ, Klenerman P et al. Positive selection of HIV-1 cytotoxic T lymphocyte escape variants during primary infection. *Proc Natl Acad Sci USA* 1997: **94**: 1890–5.
15. Jin X, Bauer DE, Tuttleton E et al. Dramatic rise in plasma viremia after CD8(+) T cell depletion in simian immunodeficiency virus-infected macaques. *J Exp Med* 1999: **189**: 991–8.
16. Schmitz J, Kuroda EMJ, Santra S et al. Control of viremia in simian immunodeficiency virus infection by CD8+ lymphocytes. *Science* 1999: **283**: 857–60.
17. Rosenberg ES, Altfeld M, Poon SH et al. Immune control of HIV-1 after early treatment of acute infection. *Nature* 2000: **407**: 523–6.
18. Geels MJ, Cornelissen M, Schuitemaker H et al. Identification of sequential viral escape mutants associated with altered T-cell responses in a human immunodeficiency virus type 1-infected individual. *J Virol* 2003: **77**: 12430–40.
19. Phillips RE, Rowland-Jones S, Nixon DF et al. Human immunodeficiency virus genetic variation that can escape cytotoxic T cell recognition. *Nature* 1991: **345**: 453–9.
20. Moore CB, John M, James IR, Christiansen FT, Witt CS, Mallal SA. Evidence of HIV-1 adaptation to HLA-restricted immune responses at a population level. *Science* 2002: **296**: 1439–43.
21. Clayton J, Lonjou C, White W. Alleles and haplotype frequencies for HLA loci in various ethnic groups. In: Charron D, ed. *HLA. Genetic Diversity of HLA: Functional and Medical Implications, Vol. I. Paris: EDK, 1997, 665–820.*
22. Takiguchi M, Matsuda T, Tomiyama H. Polarity of the P1 anchor residue determines peptide binding specificity between HLA-A*3101 and HLA-A*3303. *Tissue Antigens* 2000: **56**: 501–6.
23. Hossain MS, Tomiyama H, Inagawa T, Ida S, Oka S, Takiguchi M. Identification and characterization of HLA-A*3303-restricted, HIV type 1 Pol- and Gag-derived cytotoxic T cell epitopes. *AIDS Res Hum Retroviruses* 2003: **19**: 503–10.
24. Ikeda-Moore Y, Tomiyama H, Miwa K et al. Identification and characterization of multiple HLA-A24-restricted HIV-1 CTL epitopes: strong epitopes are derived from V regions of HIV-1. *J Immunol* 1997: **159**: 6242–52.
25. Satoh M, Takamiya Y, Oka S, Tokunaga K, Takiguchi M. Identification and characterization of HIV-1-specific CD8+ T cell epitopes presented by HLA-A*2601. *Vaccine* 2005: **23**: 3783–90.
26. Tomiyama H, Sakaguchi T, Miwa K et al. Identification of multiple HIV-1 CTL epitopes presented by HLA-B*5101 molecules. *Hum Immunol* 1999: **60**: 177–86.
27. Sette A, Vitiello A, Reherman B et al. The relationship between class I binding affinity and immunogenicity of potential cytotoxic T cell epitopes. *J Immunol* 1994: **153**: 5586–92.
28. Safrit JT, Andrews CA, Zhu T, Ho DD, Koup RA. Characterization of human immunodeficiency virus type 1-specific cytotoxic T lymphocyte clones isolated during acute seroconversion: recognition of autologous virus sequences within a conserved immunodominant epitope. *J Exp Med* 1994: **179**: 463–72.
29. Takahashi K, Dai L, Fuerst TR et al. Specific lysis of human immunodeficiency virus type 1-infected cells by a HLA-A3.1-restricted $CD8^+$ cytotoxic T-lymphocyte clone that recognized a conserved peptide sequence within the gp41 subunit of the envelope protein. *Proc Natl Acad Sci USA* 1991: **88**: 10277–81.
30. Dong T, Boyd D, Rosenberg W et al. An HLA-B35-restricted epitope modified at an anchor residue results in an antagonist peptide. *Eur J Immunol* 1996: **26**: 335–9.
31. Goulder PJ, Reid SW, Price DA et al. Combined structural and immunological refinement of HIV-1 HLA-B8-restricted cytotoxic T lymphocyte epitopes. *Eur J Immunol* 1997: **27**: 1515–21.
32. Jin X, Roberts CG, Nixon DF et al. Identification of subdominant cytotoxic T lymphocyte epitopes encoded by autologous HIV type 1 sequences, using dendritic cell stimulation and computer-driven algorithm. *AIDS Res Hum Retroviruses* 2000: **16**: 67–76.
33. Falk K, Rotzschke O, Takiguchi M et al. Peptide motifs of HLA-A1, -A11, -A31, and -A33 molecules. *Immunogenetics* 1994: **40**: 238–41.
34. Tokunaga K, Ishikawa Y, Ogawa A et al. Sequence-based association analysis of HLA class I and II alleles in Japanese supports conservation of common haplotypes. *Immunogenetics* 1997: **46**: 199–205.
35. Frahm N, Goulder JP, Brander C. Broad HIV-1 specific CTL responses reveal extensive HLA class I binding promiscuity of HIV-derived, optimally defined CTL epitopes. In: Korber B, Brander C, Haynes B et al., eds. *HIV Molecular Immunology 2003. Los Alamos, NM: Los Alamos National Laboratory, Theoretical Biology and Biophysics*, 2004, 3.
36. Bahraoui E, Yagello M, Billaud JN et al. Immunogenicity of the human immunodeficiency virus (HIV) recombinant nef gene product. Mapping of T-cell and B-cell epitopes in immunized chimpanzees. *AIDS Res Hum Retroviruses* 1990: **6**: 1087–98.

分担研究者　松下　修三

発表者氏名	論文タイトル名	発表誌名	巻号	ページ	出版年
Matsushita S, Yoshimura K, Kimura T, Kamihira A, Takano M, Eto K, Shirasaka T, Mitsuya H, and Oka S.	Spontaneous recovery of hemoglobin and neutrophil levels in Japanese patients on a long-term Combivir® containing regimen.	***J Clin Virol***	33	188-193	2005
Sakaguchi N, Kimura, **Matsushita S**, Fujimura S, Shibata J, Araki M, Sakamoto T, Minoda S, and Kuwahara K.	Generation of high-affinity antibody against T cell-dependent antigen in ganp gene-transgenic mouse.	***Immunol***	174	4485-4494	2005

ELSEVIER

Journal of Clinical Virology 33 (2005) 188–193

JOURNAL OF CLINICAL VIROLOGY

www.elsevier.com/locate/jcv

Spontaneous recovery of hemoglobin and neutrophil levels in Japanese patients on a long-term Combivir® containing regimen

Shuzo Matsushita[a,d,*], Kazuhisa Yoshimura[a,d], Tetsuya Kimura[a], Asako Kamihira[b], Misao Takano[c], Kenichiro Eto[d], Takuma Shirasaka[b], Hiroaki Mitsuya[d], Shinichi Oka[c]

[a] *Division of Clinical Retrovirology and Infectious Diseases, Center for AIDS Research, Kumamoto University, 2-2-1 Honjo, Kumamoto 860-0811, Japan*
[b] *Department of Immunological and Infectious Diseases, Osaka National Hospital, Osaka 540-0006, Japan*
[c] *AIDS Clinical Center, International Medical Center of Japan, Tokyo 162-8655, Japan*
[d] *Department of Infectious Diseases, Kumamoto University School of Medicine, Kumamoto 860-8556, Japan*

Received 11 August 2004; accepted 3 November 2004

Abstract

Objective: In order to evaluate long-term toxicity of Combivir, we retrospectively reviewed clinical records of HIV-1 infected cases under treatment with Combivir-containing regimen and we analyzed the clinical data compared to other NRTIs-containing regimens.
Study design: A total of 55 patients who were on Combivir and 39 on a control regimen were examined.
Results: After starting treatment with Combivir-containing regimens viral load and $CD4^+$ T-cell count improved as well as the control group. Rates of adverse events in Combivir group and ZDV (400 mg/day) + 3TC group were 50.9% (28/55) and 60% (12/20), respectively. Some of these Japanese patients who started Combivir regimen as a first-line HAART (primary Combivir group) showed some decrease in hemoglobin levels or neutrophil counts within 6 months. However, a significant recovery of these indices of hematological toxicities occurred in patients who continued the regimen for 18–24 months.
Conclusion: Our findings suggest that the safety of 600 mg of ZDV is similar to 400 mg/day of ZDV and the existence of mechanisms that compensate for anemia and for the neutropenia associated with long-term use of Combivir.

Keywords: Combivir; Zidovudine; Lamivudine; Hemoglobin; Neutrophil; Long-term treatment

1. Introduction

Prognosis of HIV infections dramatically improved after introduction of highly active anti-retro viral therapy (HAART). However, the occurrence of adverse events and drug resistance during long-term use of anti-retrovirals are now big issues (Yeni et al., 2002; Dieleman et al., 2002). Present HAART also has a problem to maintain a high adherence because of the pill burden and patients' quality of life is affected. Combivir® is a fixed dose combination tablet containing zidovudine (ZDV) and lamivudine (3TC) (Eron et al., 2000). Each tablet contains 300 mg of ZDV and 150 mg of 3TC and has been widely used as a nucleoside reverse transcriptase inhibitor (NRTI) component of HAART against HIV-1 infection.

HIV infection and AIDS are known to be associated with a significant hematological toxicity, including anemia, neutropenia, and thrombocytopenia (Moses et al., 1998). In addition, studies with zidovudine have shown that this drug may compound the hematological toxicity of HIV and lead to an independent development of anemia and neutropenia (Wilde and Langtry, 1993). Consistent with these observations, the incidence of anemia or neutropenia in mildly or asymptomatic adults treated with zidovudine was between 1.1% and 9.7%, whereas in adults with AIDS or the AIDS related complex it ranged from 15% to as high as 61% (Wilde

* Corresponding author. Tel.: +81 96 373 6536; fax: +81 96 373 6537.
E-mail address: shuzo@kaiju.medic.kumamoto-u.ac.jp (S. Matsushita).

1386-6532/$ – see front matter © 2004 Elsevier B.V. All rights reserved.
doi:10.1016/j.jcv.2004.11.002

and Langtry, 1993). In Japan, many physicians prescribe low dose ZDV such as 400 mg/day to avoid drug-induced anemia and neutropenia even though the standard dose of ZDV is 500–600 mg/day in United States (Kimura et al., 1992, 1998). Given the dose-dependent nature of these adverse effects, they are concerned about increased risk of hematological toxicity using Combivir that contains 600 mg of ZDV as the daily dose for Japanese patients who have lower body weights compared to patients in United States. Moreover, long-term consequence of the hematological toxicity resulting from continuous use of Combivir has not been well defined. We retrospectively reviewed clinical records of HIV-1 infected cases under treatment of Combivir-containing regimen used in three hospitals in Japan and we analyzed clinical data cross-sectionally to evaluate long-term toxicity of Combivir.

2. Patients and methods

HIV-1 positive Japanese patients were recruited from Kumamoto University Hospital, Osaka National Hospital and International Medical Center of Japan from June 1999 (after the Combivir launch) until June 2003. The clinical record was investigated in a retrospective manner. All collected cases were separated into four groups, as follows;

Primary Combivir Group (PCV): started Combivir as a first-line HAART.
Secondary Combivir Group (SCV): changed to Combivir from other NRTIs.
Primary Control Group (PCO): started NRTIs (except for Combivir) as a first-line HAART.
Secondary Control Group (SCO): changed to NRTIs except Combivir from other NRTIs.

We checked hemoglobin levels and neutrophil counts to examine the influence on hematological toxicity of ZDV every 6 months. We analyzed the data that could be followed over 18 months for removing various biases such as drop out cases with abnormal laboratory test values. Moreover, we also checked the HIV-RNA, $CD4^+$ T-cell counts and other laboratory test data every 6 months. We also checked any adverse events. This study was done under the approval of the Institutional Review Board of the Kumamoto University Hospital, Japan. All participants provided written informed consent.

3. Results

3.1. Patients' characteristics

Of the 94 data on subjects were 55 who were on Combivir (PCV: 27, SCV: 28) and 39 were on control regimens (PCO: 29, SCO: 10). The NRTIs used in the control group included of 20 cases of ZDV (400 mg/day) + 3TC, 18 cases of stavudine (d4T) + 3TC and one case of d4T + didanosine (ddI). Patients' characteristics are shown in Table 1. A couple of factors are statistically different such as the sex ($p < 0.01$: Fisher's exact test), weight ($p < 0.05$: Student's t-test) and Karnofsky score ($p = 0.0062$: Student's t-test) between Combivir group and control group. Combivir was likely to be used for patients with a higher baseline weight and the males. The mean viral load at baseline in Combivir group was $10^{3.9}$ copies/mL and for the control group was $10^{4.1}$ copies/mL. There was no statistical difference between the groups. The baseline $CD4^+$ T-cell counts in Combivir group were higher than in the control group significantly ($393/mm^3$ versus $263/mm^3$; $p = 0.0101$: Student's t-test). Most patients were prescribed efavirenz (EFV) or nelfinavir (NFV) as a concomitant drug. Fifty-two percent of all patients were on EFV and 16% were taking NFV. The Combivir group had more combination cases with EFV than did the control group, because these two drugs approved for use in Japan at the same period have similar characteristics such as small pill counts and frequency of ingestion.

3.2. Effects on hemoglobin levels

To avoid biases in the data resulting from inclusion of patients with a shorter time follow up, including drop out cases, we focused on the patients that could be followed for over 18 months. Mean hemoglobin levels at baseline of Combivir group (PCV group: 13.9 g/dL, SCV group: 14.2 g/dL) were higher than for the control group (PCO group: 13.1 g/dL, SCO group: 13.7 g/dL) (Fig. 1A). It seems Combivir was likely to give to those with a lesser risk of anemia. We divided patients in PCV group into two sub-groups such as hemoglobin level decreased (sub-group A; $n = 10$) and not changed or increased (sub-group B: $n = 8$) at 6 months after starting Combivir. Fig. 1B shows a trend of hemoglobin levels in sub-group A. Each hemoglobin level at 6, 12, 18 and 24 months after starting treatment decreased significantly compared to baseline ($p < 0.005$, $p < 0.005$, $p < 0.005$ and $p < 0.05$, respectively; Wilcoxon matched pairs signed rank test). However, the decreased hemoglobin levels at 6 months gradually recovered to the baseline level despite continuation of the same regimen. The hemoglobin level at 18, 24 months increased significantly compared to 6-month values ($p < 0.05$ and $p < 0.005$, respectively). On the other hand, the hemoglobin level of sub-group B did not decrease for 18–30 months of follow up period (data not shown). The difference of background between sub-groups A and B was baseline level of hemoglobin and hematocrit. These levels in sub-group A were higher than for sub-group B statistically (14.9 ± 1.2 versus 12.6 ± 0.7; $p < 0.001$, 44.4 ± 3.2 versus 37.4 ± 2.0; $p < 0.001$, Student's t-test).

3.3. Effects on neutrophil counts

The trend of mean neutrophil counts was similar to counts for hemoglobin levels. Mean neutrophil counts of all groups

Table 1
Baseline characteristics

	Combivir group (PCV + SCV) ($n = 55$)	Control group (PCO + SCO) ($n = 39$)	p-value
Sex (male/female)	54/1	32/7	0.00815[a]
Age	35.9 ± 9.5 (22–68)	38.6 ± 10.7 (23–78)	0.2117[b]
Weight (kg)	64.6 ± 10.8 (47.0–91.6)	59.6 ± 11.2 (36.4–81.0)	0.0303[b]
Hemophilia			
Non	48	32	0.562[a]
A	5	7	
B	2	0	
Baseline VL (log)			
<2.6	19	11	0.4432[b]
2.6–3	1	1	
3–4	6	4	
4–5	11	13	
>5	15	10	
Unknown	3	0	
Mean ± S.D.	3.9 ± 1.2	4.1 ± 1.2	
Range	2.6–5.9	2.6–5.9	
Baseline CD4 count			
<200	14	14	0.0101[b]
200–500	25	19	
>500	13	5	
Unknown	3	1	
Mean ± S.D.	393 ± 265	263 ± 179	
Range	1–1132	5–607	
CDC class			
A1	5	3	0.8064[c]
A2	22	17	
A3	6	13	
B1	2	0	
B2	3	0	
B3	2	5	
C1	3	0	
C3	12	11	
Karnofsky score			
20%	0	1	0.0062[b]
40%	0	2	
50%	0	1	
60%	1	0	
70%	0	1	
80%	4	6	
90%	11	8	
100%	39	20	
Mean ± S.D.	95.8 ± 7.9	87.7 ± 19.4	

[a] Fisher' exact test.
[b] Student's t-test.
[c] Wilcoxon 2-sample test.

were over 2000/mm^3 and did not have statistically change from the baseline during the follow up period (Fig. 1C). We separated subjects in the PCV group into two sub-groups as well as for hemoglobin levels to examine the toxicity of Combivir to neutrophils. In the sub-group C ($n = 10$) those with mean neutrophil counts decreased and the sub-group D ($n = 7$) included subjects with no changes or increased neutrophil counts at 6 months after being on Combivir. Fig. 1D shows the trend of the neutrophil counts in sub-group C. Neutrophil counts at 6, 12, 18 and 24 months after starting the treatment decreased significantly compared to baseline ($p < 0.005$, $p < 0.05$, $p < 0.05$ and $p < 0.05$, respectively; Wilcoxon matched pairs signed rank test). However, the decreased neutrophil counts gradually recovered as did hemoglobin levels. The mean neutrophil counts at 18 months increased significantly compared to data at 6 months ($p < 0.05$; Wilcoxon matched pairs signed rank test).

3.4. Effects on other laboratory test value

MCV values at baseline for the secondary treatment group such as SCV group and SCO group were higher than for pri-

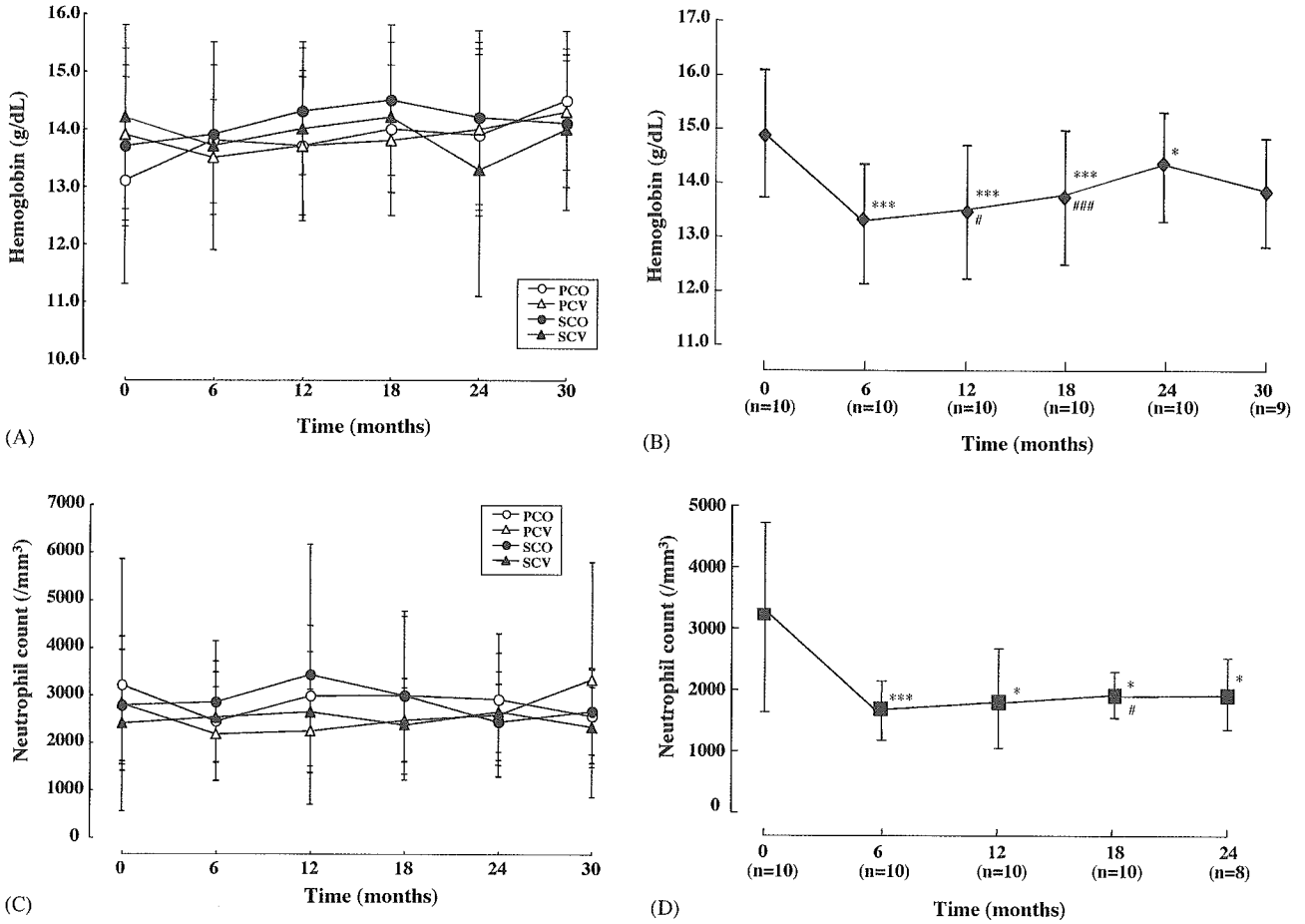

Fig. 1. Recovery after transient suppression of hemoglobin and neutrophil levels in patients with long-term use of Combivir. (A) Mean hemoglobin levels did not change significantly in all groups during each treatment. The baseline hemoglobin level in the Combivir group (PCV + SCV) was higher than in controls (PCO + SCO). (B) Mean hemoglobin levels at 6, 12, 18 and 24 months after start of treatment decreased significantly compared to baseline in the subgroup A of PCV group ($n = 10$). However the decreased hemoglobin level gradually reverted to the baseline levels despite continuation of the same regimen. Hemoglobin levels at 12 and 18 months were significantly high compared to findings at 6 months. (Wilcoxon matched pairs signed rank test; $^{*,\#}p < 0.05$, $^{***,\#\#\#}p < 0.005$). (C) Mean neutrophil counts did not change significantly in all groups during each treatment. (D) Mean neutrophil counts at 6, 12, 18 and 24 months after beginning treatment decreased significantly compared to baseline in sub-group C of PCV group ($n = 10$). However, the neutrophil counts gradually reverted to baseline levels despite continuation of the same regimen. The neutrophil counts at 18 months was significantly high compared to that of 6 months (Wilcoxon matched pairs signed rank test; $^{*,\#}p < 0.05$, $^{***}p < 0.005$).

mary treatment groups such as PCV group and PCO group. It seems ZDV or d4T in the secondary treatment group affected red blood cell counts. However, after starting each treatment, MCV values increased and became high at around 110/mm^3 in all groups (Fig. 2A). Other laboratory test values did showed no notable changes (data not shown).

3.5. Adverse events

The most common adverse events in each group were nausea/vomiting, dizziness and malaise. Anemia was observed in two in the Combivir group and one in the control group. Discontinuing each treatment led to elimination of these adverse effects. The anemia in two in the Combivir group was observed 2 months after their starting treatment, and that in one in the control group was evident as early as the eighth day. The occurrence of anemia in the control group was on ZDV 400 mg/day + 3TC. The frequency of anemia in the Combivir group was 3.6% (2/55) and similar to that in the control group {2.6% (1/39)}. The 20 in the control group on ZDV + 3TC regimen were on a ZDV 400 mg/day. We compared the safety profile of ZDV 600 mg/day to ZDV 400 mg/day. Adverse events rate of Combivir was 50.9% (28/55) and 60.0% (12/20) of AZT + 3TC group. Moreover, the number who discontinued Combivir group was 7 (12.7%) and that in ZDV + 3TC group was 5 (25.0%). In the SCV group, nineteen were changed to Combivir from ZDV 400 mg/day + 3TC. There were six with some adverse events and these were similar to other groups' events. These observations suggest that increasing the ZDV dose to 600 mg/day does not affect the incidence of adverse events. In addition there were no concomitantly used drugs that could affect pharmacokinetic parameters of ZDV and enhance its toxicity.

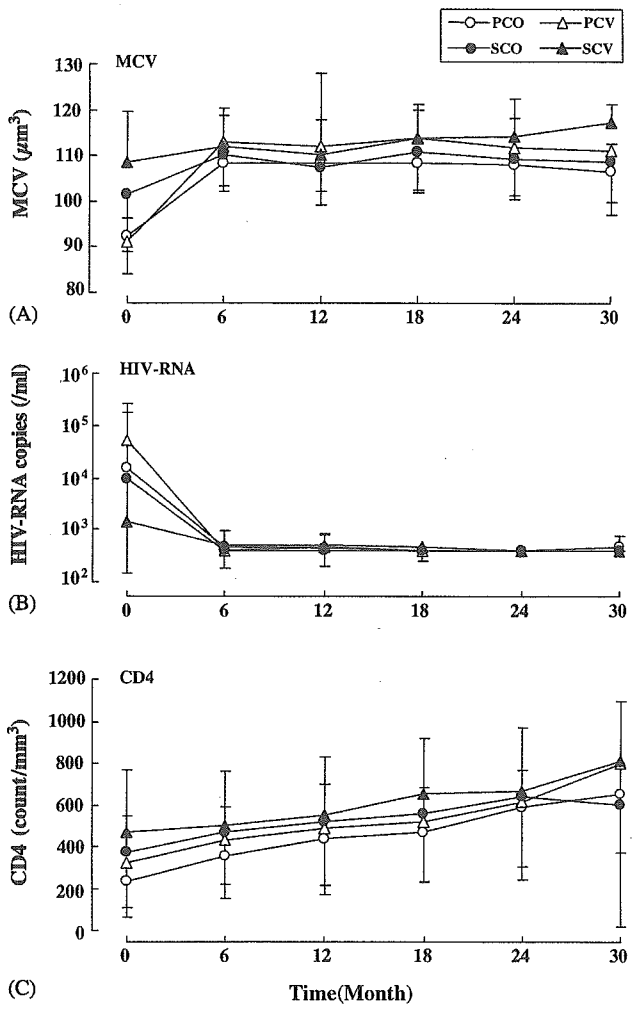

Fig. 2. Changes in MCV values, HIV RNA level and CD4$^+$ T cell counts in each group of patients. (A) MCV values for the secondary treatment group such as SCV and SCO group were higher than for primary treatment groups such as PCV and PCO group at baseline. However, after starting each treatment, MCV values increased and became high at around 110/mm^3 in all groups. (B) Mean HIV RNA level in all groups of treatment decreased compared to baseline significantly ($p < 0.05$–$p < 0.001$; Wilcoxon matched pairs signed rank test). (C) Mean CD4$^+$ T cell counts in all groups of treatment increased significantly compared to the baseline ($p < 0.05$–$p < 0.001$; Wilcoxon matched pairs signed rank test).

3.6. Effects on viral load and CD4$^+$ T-cell counts

Baseline viral load in the primary treatment group (PCV + PCO) was higher than in the secondary treatment group (SCV + SCO). Mean baseline viral loads of each group were $10^{4.6}$ copies/mL (PCV), $10^{4.0}$ copies/mL (PCO), $10^{3.0}$ copies/mL (SCV) and $10^{3.7}$ copies/mL (SCO), respectively. However, after starting each treatment, HIV RNA was not detectable in serum samples from in each group (VL < 50 or <400 copies/mL) (Fig. 2B). Baseline CD4$^+$ T-cell count in the SCV group was 518/mm^3 and higher than other groups (PCV: 304/mm^3, SCO: 345/mm^3, PCO: 277/mm^3) significantly ($p < 0.001$; Student's t-test) (Fig. 2C). This result suggests effective treatment with the previous combination for the SCV group. CD4$^+$ T-cell counts during each treatment increased significantly ($p < 0.05$–$p < 0.001$; Wilcoxon matched pairs signed rank test) and reached over 600/mm^3 at 30 months in all groups (Fig. 2C).

4. Discussion

The nucleoside reverse transcriptase inhibitor (NRTI) was first developed as an anti-HIV drug. However, the appropriate dosage was unclear because this type of drug is only active after being phosphorylated inside cells. A daily dose of 400 mg of ZDV has been widely used in Japan because anemia and neutropenia occurred frequently in cases of ingesting a higher dose (800 mg/day) than did 400 mg/day of ZDV in a clinical trial conducted in Japan (Kimura et al., 1992). Bone marrow toxicity associated with AZT such as macrocytic anemia and neutropenia has been frequently reported for the patients treated with a higher dose of ZDV mono therapy (Richman et al., 1987). Given the dose-dependent nature of these adverse effects, Japanese health care providers have some hesitance to prescribe Combivir that contains 600 mg of ZDV, as the daily dose. Data on four patients with severe anemia associated with Combivir have also been reported (Sibery et al., 2003). To evaluate the long-term toxicity of Combivir, we reviewed clinical records of HIV-1 infected Japanese patients on treatment with Combivir-containing regimen.

The results in this retrospective study showed that anemia and adverse events occurred at comparable frequency in each group of patients. Consistent with previous reports (Hester and Peacock, 1998; Tseng et al., 1998) these adverse events occurred in less than a few months after starting each treatment. The frequency of anemia in the Combivir group was only 3.7% (2/54), and it was similar to that for ZDV 400 mg/day + 3TC group (5.0%) group. In other words there was no difference in these groups with respect to the frequency of anemia by the difference in the dose of ZDV. It is also of note that the efficacy of Combivir was comparable to that of 400 mg of ZDV of four times a day with a twice a day dosing of 3TC. However, we have to take into account the fact that Combivir was prescribed for heavy weight patients. And such may mask the occurrence of adverse events as well as the difference in efficacy.

We observed a certain degree of decrease in hemoglobin levels and neutrophil counts in the subgroups of patients in PCV (subgroups A and C, respectively). Interestingly, a gradual recovery of these hematological toxicities occurred despite the continuation of Combivir containing regimens. The mechanism whereby the risk of hematological toxicity associated with increasing ZDV dosages may be related to the intracellular accumulation of the toxic metabolite zidovudine monophosphate (AZTMP) (Tornevik et al., 1995). AZTMP interferes with both cellular DNA synthesis and exonuclease-catalyzed removal of ZDV from host cell DNA (Sommadossi et al., 1989; Harrington et al., 1993). In addition, at clinically

relevant concentrations, AZTMP acts as a potent inhibitor of the transport of pyrimidine nucleotide sugars into the Golgi complex, thereby inhibiting protein glycosylation and altering glycosphingolipid synthesis (Yan et al., 1995). Therefore, AZTMP may elicit cytotoxic effects on rapidly growing erythrocytes and neutrophil precursors, both by interfering with nuclear DNA replication and by compromising the function of membrane receptors involved in receiving of extracellular stimuli required for cell growth and differentiation. From these observations it seems reasonable to speculate that either decrease in the intracellular concentration of AZTMP or compensatory mechanisms that improve the signal transduction for erythropoiesis and myelopoiesis mediated by cytokines contributed the recovery from hematological toxicities.

Two mechanisms may be related to the decrease in the concentration of AZTMP: altered metabolism of nucleoside analogues due to impaired nucleoside phosphorylation and increased efflux of the compounds by membrane transport mechanisms (Schuetz et al., 1999; Wijnholds et al., 2000). These mechanisms have been considered to contribute to the cellular drug-resistance (Dianzani et al., 1994; Groschel et al., 1997; Fridland et al., 2000; Turriziani et al., 2000). However, there was no evidence of treatment failure for patients in our PCV group as we found an increase in $CD4^+$ cell counts and an undetectable HIV-RNA load. Furthermore, the MCV level which is associated with the intracellular increase of AZTMP was kept high. These observations suggest that decrease in the level of AZTMP in the course of long-term treatment is unlikely although we must determine longitudinal changes of intracellular AZTMP level in precursors of blood cells in patients on Combivir treatment. Other compensatory mechanisms against the hematological toxicity may occur. An increase in erythropoietin or granulocyte-colony stimulating factor (G-CSF) levels in compensation for chronic anemia or neutropenia is another notion.

Acknowledgments

This work was supported in part by the Ministry of Health, Labor and Welfare of Japan (H-15-AIDS-001, -011, -015 and H-13-AIDS-001).

References

Dianzani F, Antonelli G, Turriziani O, Riva E, Simeoni E, Signoretti C, et al. Zidovudine induces the expression of cellular resistance affecting its antiviral activities. AIDS Res Hum Retroviruses 1994;10:1471–8.

Dieleman JP, Jambroes M, Gyssens IC, Sturkenboom MC, Stricker BH, Mulder WM, et al. Determinants of recurrent toxicity-driven switches of highly active antiretroviral therapy. The ATHENA Cohort. AIDS 2002;16:737–45.

Eron JJ, Yetzer ES, Ruane PJ, Becker S, Sawyerr GA, Fisher RL, et al. Efficacy, safety, and adherence with a twice-daily combination of lamivudine/zidovudine tablet formulation, plus a protease inhibitor, in HIV infection. AIDS 2000;14:671–81.

Fridland A, Connelly MC, Robbins BL. Cellular factors for resistance against antiretroviral agents. Antiviral Ther 2000;5:181–5.

Groschel B, Cinatl J, Cinatl Jr J. Viral and cellular factors for resistance against antiretroviral agents. Intervirology 1997;14:400–7.

Harrington JA, Reardon JE, Spector T. 3′-Azido-3′-deoxythymidine (AZT) monophosphate: an inhibitor of exonucleolytic repair of AZT terminated DNA. Antimicrob Agents Chemother 1993;37: 918–20.

Hester EK, Peacock Jr JE. Profound and unanticipated anemia with lamivudine-zidovudine combination therapy in zidovudine-experienced patients with HIV infection. AIDS 1998;12:439–40.

Kimura S, Oka S, Toyoshima T, Hirabayashi Y, Kikuchi Y, Mitamura K, et al. A randomized trial of reduced doses of azidothymidine in Japanese patients with human immunodefiency virus type 1 infection. Intern Med 1992;31:871–6.

Kimura S, Yamada K, Ito A, Mimaya J, Takamatsu J, 3TC Study Group. Phase 2 clinical study on 3TC (Lamivudine) in HIV infections. Antibiot Chemother 1998;14:1419–32.

Moses A, Nelson J, Bagby Jr GC. Review article: the influence of human immunodeficiency virus-1 on hematopoiesis. Blood 1998;91:1479–95.

Richman DD, Fischl MA, Grieco MH, Gottlieb MS, Volberding PA, Laskin OL, et al. The toxicity of azidothymidine (AZT) in the treatment of patients with AIDS and AIDS-related complex. A double-blind, placebo-controlled trial. N Engl J Med 1987;317:192–7.

Schuetz JD, Connelly MC, Sun D, Paibir SG, Flynn PM, Srinivas RV, et al. MRP4: a previously unidentified factor in resistance to nucleoside-based antiviral drugs. Nat Med 1999;5:1048–51.

Sibery MJ, Astrow A, Kempin S, Halperin I. Combivir (AZT/3TC) therapy is associated with life-threatening anemia in patients with HIV infection. Blood 2003;102:51b (Abstract 3907).

Sommadossi JP, Carlisle R, Zhou Z. Cellular pharmacology of 3-azido-3′-deoxythymidine with evidence of incorporation into DNA of human bone marrow cells. Mol Pharmacol 1989;36:9–14.

Tornevik Y, Ullman B, Balzarini J, Wahren B, Eriksson S. Cytotoxicity of 3′-azido-3′-deoxythymidine correlates with 3′-azidothymidine-5′-monophosphate (AZTMP) levels, whereas anti-human immunodeficiency virus (HIV) activity correlates with 3′-azidothymidine-5′-triphosphate (AZTTP) levels in cultured CEM T-lymphoblastoid cells. Biochem Pharmacol 1995;49:829–37.

Tseng A, Conly J, Fletcher D, Keystone D, Salit I, Walmsley S. Precipitous declines in hemoglobin levels associated with combination zidovudine and lamivudine therapy. Clin Infect Dis 1998;27:908–9.

Turriziani O, Antonelli G, Dianzani F. Cellular factors involved in the induction of resistance of HIV to antiretroviral agents. Int J Antimicrob Agents 2000;16:353–6.

Wijnholds J, Mol CA, van Deemter L, de Haas M, Scheper GL, Baas F, et al. Multidrug-resistance protein 5 is a multispecific organic anion transporter able to transport nucleotide analogs. Proc Natl Acad Sci USA 2000;97:7476–81.

Wilde MI, Langtry HD. Zidovudine. An update of its pharmacodynamic and pharmacokinetic properties, and therapeutic efficacy. Drugs 1993;46:515–78.

Yan JP, Ilsley DD, Frohlick C, et al. 3′-Azidothymidin (zidovudine) inhibits glycosylation and dramatically alters glycosphingolipid synthesis in whole cells at clinically relevant concentrations. J Biol Chem 1995;270:22836–41.

Yeni PG, Hammer SM, Carpenter CCJ, Cooper DA, Fischl MA, Gatell JM, et al. Antiretroviral treatment for adult HIV infection. 2002. Updated recommendation of the International AIDS Society-USA Panel. JAMA 2002;288:222–35.

Generation of High-Affinity Antibody against T Cell-Dependent Antigen in the *Ganp* Gene-Transgenic Mouse[1]

Nobuo Sakaguchi,[2]*¶ Tetsuya Kimura,† Shuzo Matsushita,† Satoru Fujimura,* Junji Shibata,† Masatake Araki,‡ Tamami Sakamoto,§ Chiemi Minoda,§ and Kazuhiko Kuwahara*‖

Generation of high-affinity Ab is impaired in mice lacking germinal center-associated DNA primase (GANP) in B cells. In this study, we examined the effect of its overexpression in *ganp* transgenic C57BL/6 mice (*Ganp*^{Tg}). *Ganp*^{Tg} displayed normal phenotype in B cell development, serum Ig levels, and responses against T cell-independent Ag; however, it generated the Ab with much higher affinity against nitrophenyl-chicken gammaglobulin in comparison with C57BL/6. To further examine the affinity increase, we established hybridomas producing high-affinity mAbs and compared their affinities using BIAcore. C57BL/6 generated high-affinity anti-nitrophenyl mAbs ($K_D \sim 2.50 \times 10^{-7}$ M) of IgG1/λ1 and contained the $V_H186.2$ region with W33L mutation. *Ganp*^{Tg} generated much higher affinity ($K_D > 1.57 \times 10^{-9}$ M) by usage of $V_H186.2$ as well as noncanonical V_H7183 regions. *Ganp*^{Tg} also generated exceptionally high-affinity anti-HIV-1 (V3 peptide) mAbs ($K_D > 9.90 \times 10^{-11}$ M) with neutralizing activity. These results demonstrated that GANP is involved in *V* region alteration generating high-affinity Ab. *The Journal of Immunology,* 2005, 174: 4485–4494.

The Ag-driven B cells expressing high-affinity BCR, which have been selected in secondary lymphoid organs, generate high-affinity Ab. Ag-driven B cells proliferate rapidly by the stimulation with Ag and costimulatory molecules from Th cells surrounding the germinal center (GC)[3] region, in which such B cells undergo affinity maturation of Ig V region and class switching of the C region during the response to T cell-dependent Ag (TD-Ag) in vivo (1, 2). For affinity maturation, introduction of somatic hypermutation (SHM) in the *V* region is probably essential and, in addition to this molecular alteration, the Ag-driven B cells with high-affinity BCR must be selected or further enriched during the maturation of Ag-driven B cells in GCs.

A 210-kDa germinal center-associated DNA primase (GANP) protein, bearing RNA-primase and minichromosome maintenance (MCM)3-binding activities, is up-regulated in GC B cells upon immunization with TD-Ag in vivo and is induced by the stimulation to BCR and CD40 in vitro (3, 4). The mutant mouse with *ganp* gene knockout B cells (B-*ganp*$^{-/-}$) has a severe defect in mounting high-affinity Ab responses to TD-Ag (5), suggesting that GANP is required for generation of high-affinity Ab in response to TD-Ag in vivo. However, there remained several possibilities to account for the molecular mechanism in generation of high-affinity V regions by the expression of GANP in GC B cells. GANP might augment the induction of SHM in the *V* regions, resulting in the affinity maturation of V regions during the proliferation and differentiation of Ag-driven B cells in GCs. Alternatively, GANP might be involved in the survival of the high-affinity BCR$^+$ B cells for the positive selection through the interaction of Ags captured on the follicular dendritic cell network. The GCs of the B-*ganp*$^{-/-}$ mice displayed an increase of apoptotic cells upon immunization with TD-Ag SRBC, which suggested a partial involvement of GANP in the survival of GC B cells. However, the *ganp*$^{-/-}$ B cells do not show marked abnormalities in the levels of apoptotic and proapoptotic molecules after BCR cross-linkage (5). To study the function of GANP in generation of high-affinity Ab response, it is necessary to examine whether the affinity maturation of BCR on the GC B cell is generated by the genetic alteration in the *V* region gene.

We speculated that it would be possible to generate a high-affinity Ab if we used mice with higher level GANP expression in B cells. We studied whether the transgenic mouse with increased expression of *ganp* gene could generate high-affinity Ab against TD-Ag using a model epitope of 4-hydroxy-3-nitrophenyl acetyl (NP)-hapten in the C57BL/6 background. To demonstrate the increased affinity of the Ab in detail, we established the hybridomas secreting anti-NP mAbs after immunization with NP-chicken gammaglobulin (CG) in *Ganp*^{Tg} mice. After selecting the high-affinity mAbs against NP-hapten by differential ELISA method and the BIAcore system, we examined the *V* region gene usage of the hybridomas and compared the sequences with those from wild-type C57BL/6 mice. The results suggest that the affinity maturation of BCR on GC B cells is generated by the altered V_H region usage with increased SHM in *Ganp*^{Tg} mice.

Materials and Methods

Ganp^{Tg} *mouse*

The expression construct of mouse *ganp* cDNA under the mouse Ig promoter and human Ig enhancer (6) was used for establishing the transgenic

*Department of Immunology, Graduate School of Medical Sciences, †Division of Clinical Retrovirology and Infectious Diseases, Center for AIDS Research, ‡Division of Bioinformatics, Institute of Resource Development and Analysis, Kumamoto University, and §Trans Genic, Kumamoto Japan; ¶Core Research for Evolutional Science and Technology Program, Saitama Japan; and ‖PRESTO, Japan Science and Technology Agency, Saitama, Japan

Received for publication October 26, 2004. Accepted for publication January 4, 2005.

The costs of publication of this article were defrayed in part by the payment of page charges. This article must therefore be hereby marked *advertisement* in accordance with 18 U.S.C. Section 1734 solely to indicate this fact.

[1] This work was supported by Special Coordination Funds for Promoting Science and Technology from the Ministry of Education, Culture, Sports, Science and Technology of Japan, Matching Funds from New Energy and Industrial Technology Development Organization, and grants from the Core Research for Evolutional Science and Technology Program, Japan Science and Technology Agency.

[2] Address correspondence and reprint requests to Dr. Nobuo Sakaguchi, Department of Immunology, Graduate School of Medical Sciences, Kumamoto University, 1-1-1, Honjo, Kumamoto 860-8556, Japan. E-mail address: nobusaka@kaiju.medic.kumamoto-u.ac.jp

[3] Abbreviations used in this paper: GC, germinal center; GANP, germinal center-associated DNA primase; NP, 4-hydroxy-3-nitrophenyl acetyl; SHM, somatic hypermutation; TD-Ag, T cell-dependent Ag; MCM, minichromosome maintenance; CG, chicken gammaglobulin; KLH, keyhole limpet hemocyanin; TNP, 2,4,6-trinitrophenyl; LTR, long terminal repeat.

0022-1767/05/$02.00

mouse by the standard procedure. Mice were screened for the transgene by PCR using *ganp* 1–5′ primer (5′-TCCCGCCTTCCAGCTGTGAC-3′) and *ganp* 1–3′ primer (5′-GTGCTGCTGTGTTAT GTCCT-3′) and Southern blot analysis using *ganp* probe A (1143–2193 nt) of tail genomic DNAs. The *Ganp*^{Tg} mice that express 1.5- to 2.0-fold increase of *ganp* gene grew normally under specific pathogen-free condition and were immunized with Ags. *Ganp* transcripts were detected by two primers (*ganp* 1–5′ and *ganp* 1–3′) in comparison with *β-actin* control (5). All mice were maintained in the Center for Animal Resources and Development (Kumamoto University, Kumamoto, Japan).

Flow cytometric analysis

Single-cell suspensions from lymphoid organs were stained with each biotin-labeled mAb in combination with FITC-conjugated streptavidin (Amersham Biosciences) and PE-conjugated mAbs. Lymphoid cells were analyzed by FACSCalibur (BD Biosciences) using CellQuest software.

In vitro proliferation assay

Purified B cells were cultured for 48 h at a density of 2×10^5 cells/well in 96-well microtiter plates in RPMI 1640 medium containing 10% heat-inactivated FCS (JRH Biosciences), 2 mM L-glutamine, and 5×10^{-5} M 2-ME. The cells stimulated with or without various mitogenic stimulants were pulsed with 0.2 μCi/well of [^{3}H]thymidine (ICN Pharmaceuticals) for 16 h before harvesting, and the incorporated radioactivity was measured by scintillation counter. Stimulatory reagents were affinity-purified goat anti-mouse μ-chain-specific Ab ($F(ab')_2$, 10 μg/ml; ICN Pharmaceuticals), rat anti-mouse CD40 mAb (LB429, 10 μg/ml) (4), and LPS (10 μg/ml; Sigma-Aldrich).

Immunohistochemistry

The 8-μm sections of spleen from SRBC-immunized mice were lightly fixed with acetone. Slides were blocked with 3% BSA in PBS-Tween 20

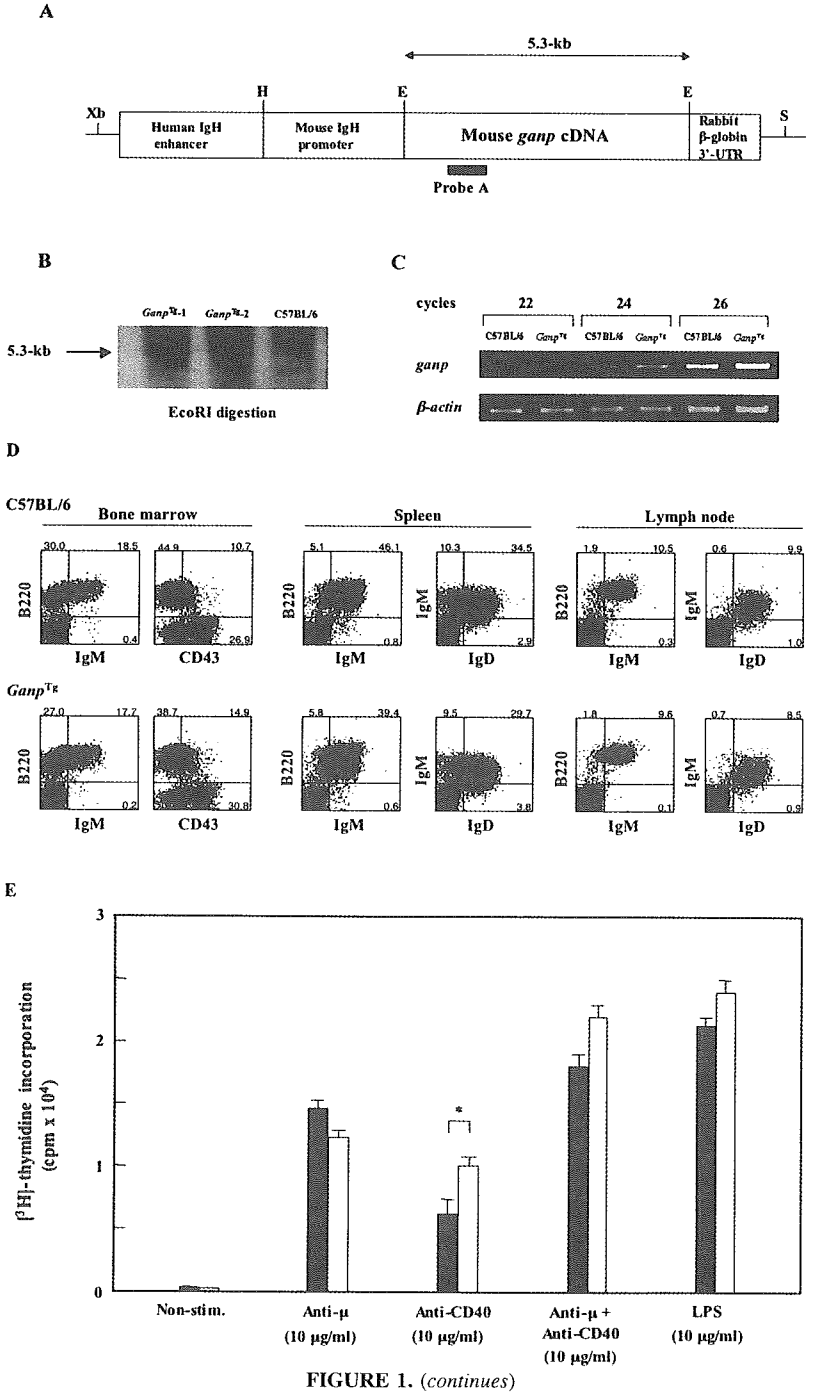

FIGURE 1. Generation of transgenic mice that overexpress the *ganp* gene in B cells. *A*, A schematic diagram of construct for *Ganp*^{Tg} under the human Ig enhancer, mouse Ig promoter, and followed by rabbit β-globin 3′-untranslated region (UTR). The construct contains restriction enzyme sites: Xb, *Xba*I; H, *Hin*dIII; E, *Eco*RI; and S, *Sal*I. The probe for Southern blot analysis (probe A) is indicated. *B*, Detection of the *ganp* transgene by Southern blot analysis. Southern blot analysis with *Eco*RI-digested genomic DNAs of *Ganp*^{Tg} displayed a 5.3-kb band hybridized with probe A. *C*, Up-regulation of *ganp* transcripts in B cells from *Ganp*^{Tg}. Semiquantitative PCR was performed using the primers *ganp* 1–5′ and *ganp* 1–3′, in comparison with *β-actin* transcripts. From densitometer analysis, *ganp* transcripts in B cells from *Ganp*^{Tg} showed an 80% increase in comparison with C57BL/6 mice. *D*, Flow cytometric analysis. Bone marrow, spleen, and lymph node cells from 8-wk-old C57BL/6 and *Ganp*^{Tg} were analyzed with indicated markers. *E*, In vitro proliferation assay of purified B cells from *Ganp*^{Tg}. [^{3}H]Thymidine incorporation was measured in the presence or absence of B cell mitogenic stimulants in C57BL/6 mice (■) and *Ganp*^{Tg} mice (□). The representative data are shown from four independent experiments. *, $p < 0.05$. *F*, Kinetics of GC formation after TD-Ag in *Ganp*^{Tg}. C57BL/6 and *Ganp*^{Tg} mice were immunized by SRBC. At day 10 or day 14, the sections were doubly immunostained with peanut agglutinin (brown) and IgD (blue). Arrows indicate GCs. *G*, T cell-independent Ag (type II)-specific or TD-Ag-specific immune responses in *Ganp*^{Tg}. Sera from mice immunized with TNP-Ficoll or TNP-KLH were collected at day 14. TNP-specific Ab titers were measured by ELISA. C57BL/6 mice (●) and *Ganp*^{Tg} mice (○) are indicated. *H*, Relative affinity of serum Abs in *Ganp*^{Tg}. Sera from C57BL/6 and *Ganp*^{Tg} mice immunized with NP-CG were collected at days 14 and 28. The NP_2 to NP_{17} ratios of anti-NP IgG1 were measured by ELISA. *I*, W33L mutation of $V_H186.2$ transcripts from C57BL/6 and *Ganp*^{Tg} mice. Mice were i.p. immunized by 20 μg of alum-precipitated NP-CG. $V_H186.2$ transcripts of γ1-isotype were amplified by RT-PCR and cloned into pBluescript vector for sequencing. The calculated percentage from sequence data was shown in C57BL/6 (■) and *Ganp*^{Tg} (□) mice. *, $p < 0.05$.

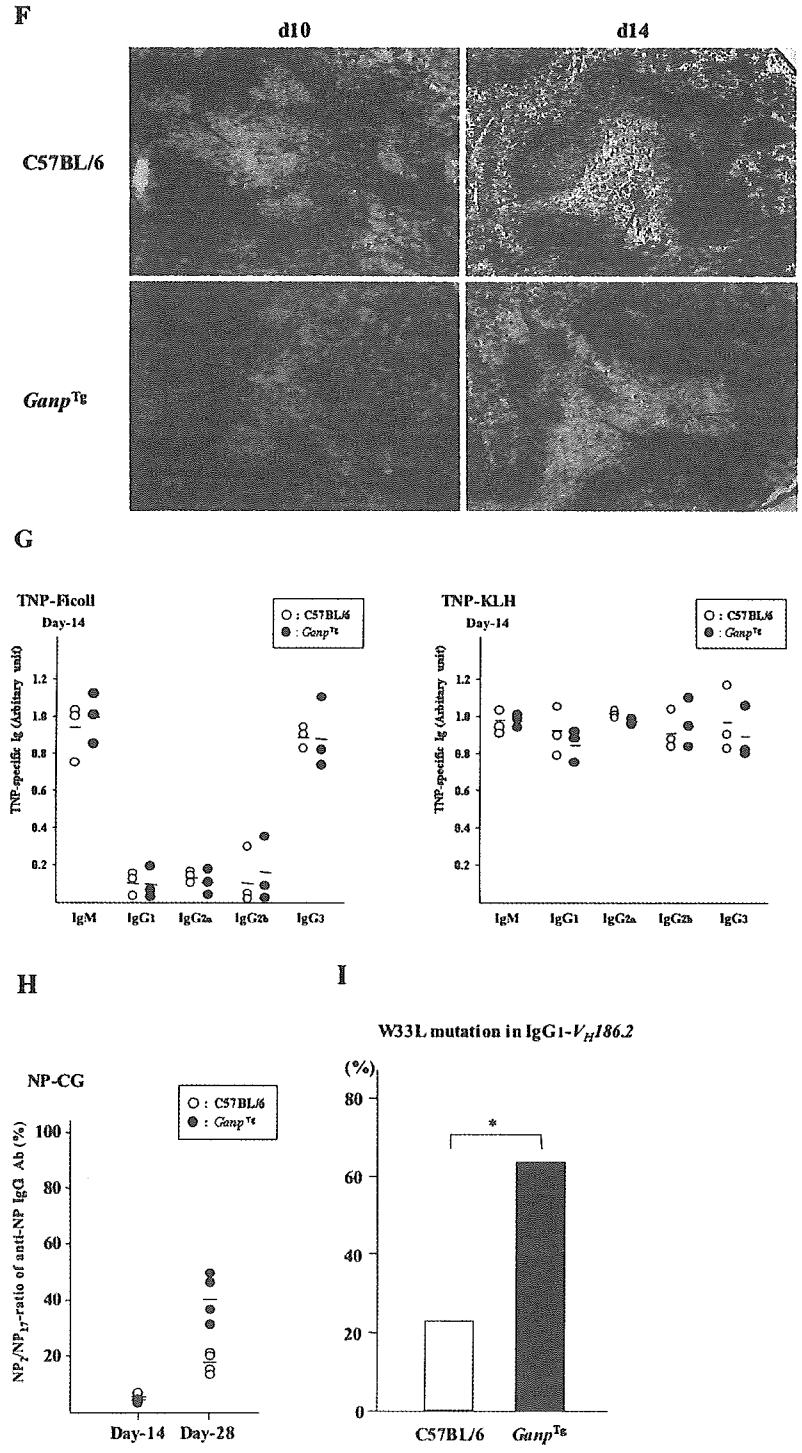

FIGURE 1. *continued.*

and incubated with anti-IgD mAb in combination with alkaline phosphatase-conjugated anti-rat IgG (ICN Pharmaceuticals). The first development step was conducted with Vector Blue kit (Vector Laboratories). For second staining, slides were incubated with biotin-conjugated peanut agglutinin (Vector Laboratories) in combination with HRP-conjugated streptavidin (Kirkegaard & Perry Laboratories), followed by 3,3′-diaminobenzidine tetrahydrochloride (Dojindo). After fixation with 1% glutaraldehyde in PBS, mounting was done by Aquatex (Merck).

Ag and immunization

2,4,6-Trinitrophenyl (TNP)-keyhole limpet hemocyanin (KLH), TNP-Ficoll, and NP_{28}-CG were purchased from Biosearch Technologies. From 20 to 100 μg of TNP-KLH and NP-CG precipitated by alum (Pierce), or 25 μg of TNP-Ficoll dissolved in PBS was injected i.p. into C57BL/6 and *Ganp*^{Tg} mice.

Measurement of Ag-specific Ab production

Five micrograms per well of TNP-BSA (Biosearch Technologies) were coated on ELISA plate, blocked with 3% BSA in PBS, and incubated with the serial-diluted sera obtained at day 14 after Ag immunization. After washing with PBS-0.1% Tween 20, the wells were incubated with biotin-conjugated isotype-specific mAb in combination with alkaline phosphatase-conjugated streptavidin (Southern Biotechnology Associates). The development was performed in the presence of substrate.

Sequence analysis of V_H186.2 gene

The *Ganp*^{Tg} mice were immunized with alum-precipitated NP-CG once as described (5). After 28 days, the spleen B cells were purified, and the total

Table I. *Affinity of the anti-NP mAb measured by BIAcore sensorgram*

mAb	H Chain	L Chain	V_H Usage	K_D, M[a]
Ganp^{Tg}				
NP-G2–6	γ1	κ	V_H 7183 family	7.05×10^{-8}
NP-G2–9	γ1	κ	V_H 7183 family	3.24×10^{-8}
NP-G2–12	γ1	λ	V_H 186.2	4.92×10^{-8}
NP-G2–14	γ1	κ	V_H 186.2	2.51×10^{-8}
NP-G2–16	γ2b	λ	V_H 186.2	1.10×10^{-7}
NP-G2–15	γ1	λ	V_H 186.2	4.12×10^{-8}
NP-G-2E4	γ2b	λ	V_H 186.2	1.57×10^{-9}
C57BL/6				
NP-W2–7	γ1	λ	V_H 186.2	1.51×10^{-7}
NP-W1–116	γ2a	λ	V_H 186.2	1.00×10^{-8}
NP-W-1B9	γ2b	λ	V_H 186.2	1.24×10^{-8}
NP-W-2D8	γ2b	λ	V_H 186.2	2.74×10^{-8}

[a] K_D was calculated using BIAcore sensorgram as described in *Materials and Methods.*

RNA was used for RT-PCR analysis with the sequence primers for IgG1-V_H*186.2* and the sequences were compared with those of C57BL/6.

Establishment of mAbs

Ag immunization was conducted with CFA as a primary immunization and then followed by boosting with IFA (4). For anti-NP-specific mAbs, NP_{28}-CG emulsified in CFA was injected i.p. and boosted after 2 wk with IFA. The mice with higher serum Ab titers were further immunized, and 3 days later, the spleen cells were obtained for cell fusion by polyethylene glycol method with mouse myeloma cell line X63 under the standard procedure (4). The fused cells were selected with hypoxanthine/aminopterin/thymidine medium on the microculture plates at the concentration of 2×10^4 cells/well with IL-6 (5 U/ml). For preparation of mAbs against the epitope of HIV-1, the peptide of the CNNTRKSIRIQRGPGRAFVYIGKI was prepared based on the amino acid sequence of the V3 loop of gp120 region of NL4-3 HIV-1 strain (prototype X4; T cell tropic) and conjugated with KLH (Merck). Sera of immunized mice were measured by ELISA using the plates coated with the HIV-1 peptide conjugated with BSA.

ELISA screening

For anti-NP mAbs, supernatants of individual wells were divided into two aliquots (each 50 μl) and measured by the differential ELISA method with two different Ag-coating as NP_2-BSA and NP_{17}-BSA (Biosearch Technologies) under the standard procedure. The mAbs binding to the Ags were captured with protein A-peroxidase (Amersham Biosciences) with the substrate (Bio-Rad). The positive signals with NP_2-BSA plates were selected in comparison with NP_{17}-BSA plates. The mAbs showing little difference (NP_2-BSA/NP_{17}-BSA > 0.5) between the two plates were cloned by limiting dilution method. Then, the positive clones were expanded for large scale to purify the mAbs in the serum-free medium (Invitrogen Life Technologies) and the mAbs were purified through protein G-Sepharose column chromatography (Amersham Biosciences) and the protein concentrations were determined by Bradford assay kit (Bio-Rad). The purities of the samples were examined by SDS-PAGE and the protein staining with Coomassie brilliant blue. The isotypes of H chain and L chain in all mAbs were determined by Isotyping kit (Dainippon Pharmaceuticals).

BIAcore assay

Affinity of the mAbs was determined by the BIAcore assay (7). The on and off rate constants (k_{on} and k_{off}) for binding of the mAbs to NP or HIV-1 V3 loop peptide were determined by BIAcore system (Biacore International). The carboxyl-methylated dextran surface of the sensor chip was activated with EDC (*N*-ethyl-*N'*-(3-dimethylaminopropyl)carbodiimide) and NHS (*N*-hydroxysuccinimide) (8). V3 loop peptide was immobilized through the free thiol group of a cysteine residue that was deliberately placed at the N terminus, by injection of 35 μl of a 20 μg/ml solution in 10 mM MES buffer (pH 6) to the EDC-NHS-activated surface that had been reacted with 2-(2-pyridinyldithio)ethaneamine. The excess disulfide groups were deactivated by the addition of cysteine. The mAbs were diluted in 10 mM HEPES (pH 7.4), 150 mM NaCl, 3.4 mM EDTA, and 0.05% (v/v) BIAcore surfactant P20 and injected over the immobilized Ag at a flow rate of 5 μl/min. The association was monitored by the increase of the refractive index of the sensor chip surface per unit time. The dissociations of the mAbs were monitored after the end of the association phase with a flow rate of 50 μl/min. Kinetic rate constants were calculated from the collected data using the Pharmacia Kinetics Evaluation software (9). The k_{on} was determined by measuring the rate of binding to the Ag at different protein concentrations.

DNA sequencing

The DNA fragments corresponding to the rearranged V_H regions were amplified using Pfu-Turbo (Stratagene) from the genomic DNA. The oligonucleotide primers are as follows (10, 11): V_H186.2 forward, 5'-CTGAC CCATGTCCCTTCTTCTCCAGCAGG-3'; V_H7183 forward, 5'-GCA GCTGGTGGAGTCTGG-3'; J_H4-3, 5'-CTCTCAGCCGGCTCCCTCA GGG-3'; Vλ1 forward, 5'-TGCTGACCAATATTGAAAAG-3'; Jλ1 reverse, 5'-AGCACCTCAAGTCTTGGAGAG-3'. For rearranged *V* κ-chain genes, the cDNA fragments were amplified using the primers designed as follows (12): V κ-Ox1 forward, 5'-ATGGATTTTCAAGTGCAGATTTTCA-3'; Vκ-21B forward, 5'-ATGGAGTCAGACACACTCCTGCTAT-3'; and Cκ reverse, 5'-TGGGAAGATGGATACAGTTGGTGCA-3'. Amplification of Cμ region was conducted with the primers: Cμ-Ex1 forward, 5'-AGTCAGTCCTTCCCAAATGTCTTCCC-3' and Cμ-Ex3 reverse, 5'-TGAAGGTTAGGATGTCTGTGGAGGG-3'. The amplified DNA fragments cloned into blunt-ended pBluescript were sequenced.

In vitro binding assay to NL4-3 envelope

293T cells were transfected with pLP-IRES2 enhanced GFP (BD Clontech) or pLP-NL4-3 envelope enhanced GFP using Effectene Transfection Reagent (Qiagen). After 36 h, cells were harvested, incubated with each anti-HIV-1 mAb in combination with allophycocyanin-conjugated goat anti-mouse IgG Ab (BD Pharmingen), and analyzed in comparison with GFP expression by FACSCalibur. The anti-CD19 mAb was purchased from BD Biosciences.

Neutralization activity assay

HIV-1 strain NL4-3 (prototype X4; T cell tropic) was propagated in PM1 cells in RPMI 1640 medium with 10% (v/v) heat-inactivated FCS, and the cell-free supernatant was collected and stored as virus stocks at −80°C. The chemiluminescent assay (Galacto-Star; Applied Biosystems) for β-galactosidase released from the HeLa-CD4$^+$/long terminal repeat (LTR)-β-galactosidase/CCR5 (MAGI/CCR5) cells were conducted as previously described (13). Tissue culture-effective dose $(TCID)_{50}$ of virus stock was predetermined with MAGI/CCR5 cells by the method of Reed and Muench (14). For the assay of neutralizing activity against HIV-1 infection, MAGI/CCR5 cells were plated in 96-well microtiter plates at a density of 1×10^4 cells/well, and on the next day, the cells were incubated with 50 μl of each mAb and 50 μl of HIV-1 solution (500 $TCID_{50}$) for 30 min at 37°C in combination with 10 μg/ml DEAE-dextran (Amersham Biosciences) in a triplicate assay. After 48 h, we measured the β-galactosidase activity for 1 s using the Galacto-Star system according to the manufacturer's protocol and showed results as percentages of the negative control.

Results

Establishment of Ganp^{Tg} *mice*

Ganp^{Tg} mice were established under control by human Ig enhancer and mouse Ig promoter in C57BL/6 background (Fig. 1, *A* and *B*), and the adult mice showed an increase of *ganp* transcripts (~2-fold) in B cells (Fig. 1*C*). *Ganp*^{Tg} mice had normal B lineage differentiation by surface marker studies of B220, IgM, and IgD on lymphoid cells in the bone marrow, spleen, and lymph nodes (Fig. 1*D*). B cell numbers and the levels of serum Igs were also normal in *Ganp*^{Tg} mice (data not shown). These results demonstrated that B cell differentiation undergoes normally in *Ganp*^{Tg} mice compared with wild-type littermates.

In vitro B cell proliferation and GC formation of Ganp^{Tg} *mice*

Next, we examined the potential of B cell proliferation of *Ganp*^{Tg} mice in vitro. *Ganp*^{Tg} mice showed comparable proliferation activities to wild-type littermates in response to anti-μ Ab, anti-μ Ab plus anti-CD40 mAb, or LPS (Fig. 1*E*). Interestingly, *Ganp*^{Tg} B cells showed augmented responses to anti-CD40 stimulation in comparison to wild-type B cells. This was only observed in the response to anti-CD40 stimulation but not in the response to anti-μ Ab or LPS stimulation, suggesting that *Ganp*^{Tg} mice augment CD40-stimulated response in vivo.